2015

Material Considerations for Development of 3D Printed Bronchial and Tracheal Stents

Nidah M. Hussain
University of South Carolina

Material Considerations for Development of 3D Printed Bronchial and Tracheal Stents

by

Nidah M. Hussain

Bachelor of Science
University of South Carolina, 2013

Submitted in Partial Fulfillment of the Requirements

For the Degree of Master of Science in

Biomedical Engineering

College of Engineering and Computing

University of South Carolina

2015

Accepted By:

David Rocheleau, Director of Thesis

Damon Kolok, Reader

Lacy Ford, Senior Vice Provost and Dean of Graduate Studies

DEDICATION

To my late paternal grandfather, Ahmad Hussain, whom I lost to an illness this stent may someday save others from, and to my maternal grandparents, Brig. Taimur Tareen and Shameem Tareen, for inspiring me from an early age to pursue knowledge, be it science, engineering, and medicine.

ACKNOWLEDGEMENTS

I would like to extend my thanks to all those hardworking individuals without whom I would not have been able to achieve this degree. In particular, I would like to thank Dr. Goodwin, from the University of South Carolina School of Medicine, for his helping me to find a good direction to take my masters project in. My wonderful thesis director Dr. Rocheleau has my gratitude for his continual guidance and sage advice throughout the course of my project, and for giving me this opportunity to gain valuable experience in mechanical engineering as well as my core biomedical training. My thanks to my fellow team members, Zach Schwab for all his design and 3D printing work, and Caroline Horton for being my liaison with the collagen team; without them this thesis would not have come together. I extend my thanks to Dr. Tarbutton, also of the University of South Carolina, for taking a chance with this project and cooperating with our lab to join biomaterial science and three-dimensional printing to make these stent prototypes possible; also a thank you to Dr. Tarbutton's graduate student Taylor Corbett for his help and trouble-shooting with our 3D printer. For my parents' unending support and encouragement, I am thankful. Also, to everyone else who helped in each of the many individual steps along the way, you all have my sincerest thanks.

ABSTRACT

Tracheobronchial malacia is a commonly under-diagnosed condition that results in difficulty breathing. The use of a tracheobronchial stent is the best course of treatment for patients whose quality of life has deteriorated due to malacia; unfortunately stents need replacing after issues with inflammation, migration, or eventual stent-breakdown resulting in fistula formation.

The purpose of this thesis is to use three-dimensional (3D) printing technology to improve on existing stents through designing and printing a bioresorbable/biodegradable tracheobronchial stent that can treat tracheobronchial malacia. This was undertaken by testing three biologically favorable materials, type I collagen, polycaprolactone (PCL), and thermoplastic polyurethane (TPU), with desirable qualities that may result in producing stents with idealized properties. These materials underwent print-compatibility testing to determine whether, following a simple tubular stent geometry similar to the Dumon silicone stent, these materials can be manufactured into a prototype stent via innovative 3D printing methods. The resulting stents were mechanically tested and compared to the industry standard Dumon silicone stent.

We demonstrated that PCL is fused deposition modeling (FDM) printing-compatible, that TPU is potentially viable as a silicone alternative that is biologically degradable, and that type I collagen can potentially be cured, using injection molding with 3D-printed molds, into a resorbable, yet stable simple stent for implantation.

TABLE OF CONTENTS

LIST OF FIGURES

CHAPTER 1. UNDERSTANDING THE PROBLEM MEDICALLY

1.1 History of Stents

This research proposes the use of three-dimensional printing technology to create implantable tracheobronchial stents. To examine this, a detailed overview of stent technology over the course of history, as well as modern technology employed today, will be presented.

Tracheobronchial malacia is a commonly under-diagnosed acquired condition in adults, occurring within an estimated 10% of the population [1]. This condition is characterized by tracheal cartilage flaccidity, a reduced anterior-posterior airway caliber, and a widened posterior membranous tracheal wall; all of which result in a temporary collapse of up to 50% or more of the trachea during eating, coughing, crying, and in extreme cases, exhaling [2, 3, 4]. Type I and Type III tracheobronchial malacia are our targets. Type I is congenital (birth defect) associated with esophageal atresia, or trachoesophageal fistula formation. Type III is acquired through inflammatory conditions like relapsing polychondritis (constant inflammation of cartilaginous structures of the nose, ears, and laryngotracheobronchial tree in particular) or chronic tracheal infections, as well as from prolonged intubation for medical reasons. Long-term treatment for this condition involves the use of stents to improve the peripheral airway clearance and improve quality of breathing.

Airway stents have been around and in use for close to 100 years. The earliest among them appearing in 1915 through the work of Gustav Killian, known as the 'Father of Bronchoscopy', and his students Brünings and Albrecht [5]. Many of the modern airway stents began as endoprosthesis developed for implantation into the vascular system. These implants were then adapted through minor modifications for central airway usage. While in the early 1900s, the first airway stents were rubber, 1933 marked the use of the first metal-based stent to treat laryngeal bony stenosis of a 2-year-old boy, by Canfield and Norton [6]. Montgomery (Fig. 1.1) closely followed this in 1965 via the creation of a silicone-rubber, T-shaped tube stent [7]. The year 1990 saw stent placement officially become an acknowledged clinical, endoscopic treatment when Dumon introduced a stent made of silicone, specialized for the trachea and bronchi [8]. Since then, Dumon silicone stents are the most commonly implanted stent types in tracheobronchial surgeries globally.

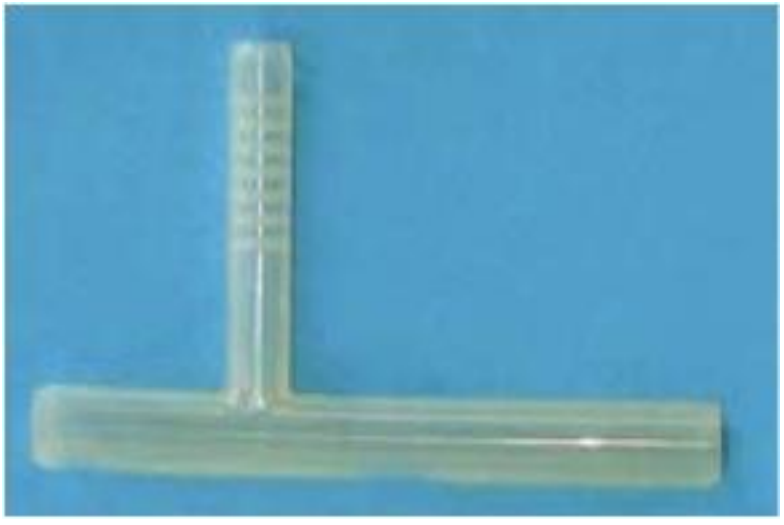

Figure 1.1. A Montgomery t-shaped tube stent.

1.2 Stents Today

Today stents like the Dumon (Fig. 1.2) are employed for three major reasons: primarily to reestablish airway patency, to provide support to weakened cartilage rings when malacia occurs, or for providing a sealant when dealing with dehiscences and fistulas in the esophagus [9]. Though not all prototypes were able to withstand the passage of time, many types of stents still exist, and can be labeled as one of four chief categories: metallic stents, covered metallic stents, polymer stents (like the Dumon), or hybrids of metal combined with polymers such as silicone (like the Dynamic stent) [9]. Metal stents tend to be made of either stainless steel or Nitinol, a nickel and titanium alloy, while polymer stents are almost primarily silicone [10]. Tissue response to a stent, and the overall outcome of an endoscopic procedure, relies heavily on the material composition of a stent and its resulting biomechanical properties [9], justifying the documented use of the abovementioned materials historically.

Figure 1.2. Silicone studded Dumon stent. Original design, product of Kaptex Healthcare Ltd.

Currently used stents are variable, depending on the nature of the particular disease intended to be treated. Each of these stents uses materials foreign to the body, although made biologically inert through modification. Much research of the following stent types and designs, principally those developed or studied by Lutz Freitag, will be a beneficial basis for future research at the University of South Carolina for a fresh, innovative range of stent materials. These are to be based instead on bioresorbable or biodegradable, polymeric materials better suited to integration and gradual breakdown in the body, bringing the idealized stent closer to reality.

1.2.1 Polymer Stents

Among the stents of today, polymer stents like the aforementioned and popular Dumon stent are most frequently used, and have become the 'de facto gold standard' of the endoscopic world [8,11]. Composed of coated silicone, the shape resembles a hollow tube with small rounded studs along the outside, while the interior surface is extremely smooth. Partly due to their simplicity, Dumon stents are extremely versatile and come in a range of sizes to allow for treatment of tracheal and bronchial stenosis from children through adults. The stent can be repositioned and replaced with ease. These stents are also prone to migration occasionally.

Figure 1.3. A self-expanding silicone Polyflex mesh stent, product of Boston Scientific.

A polyester-mesh stent, very similar in design to the Dumon, is known as the Polyflex stent (Fig. 1.3), and is even more adaptable than tube-shaped stents. This flexibility is due to its circumferential length change when local compression is applied. The addition of ‘tungsten spots’ at particular points in the mesh allow for visibility of the stent in chest X-rays. The smoothness of the surface of the Polyflex stent makes it much more prone to migration compared to other solid body tube stents. Correction of the migration risk was attempted by the addition of spike-shaped silicone structures to the exterior of the Polyflex and tested in animal models. This, however, was found to cause severe granulation of local tissue [12].

The Montgomery stents have been modified slightly from the original 1965 design, having changed the composite material and the diameters of the T-tube; they are primarily employed to treat tracheal stenosis starting from the vocal cords to further into the trachea and bronchi. Stent migration is not possible with the Montgomery, as the use of this stent necessitates a surgical tracheostomy in addition to the procedure. However, this affects patient speech capability. Lymphatic flow and blood flow are not impaired in any way, making this stent safest to employ for tracheal stenosis in this anatomical region.

1.2.2 Metal Stents

Metal stents like the Palmaz steel stent (Fig. 1.4) are mesh stents requiring balloon expansion during deployment into the tracheobronchial region; these were originally developed for use in the biliary duct and blood vessels [13], and have been successfully used in airways due to the ability to ‘mold’ the stent by the endoscopist, *in*

vivo, via manipulation with dilatation forceps or an angioplasty balloon. Epithelialization (the migration of living cells into the implant to integrate the implant into the surrounding tissue) occurs within weeks of implantation, but the stent is plastically inflexible as far as the mechanical properties are considered. Although granulation formation is far less than other metal stents, fluctuating pressure from coughing could permanently deform the stent, requiring that serious caution be exercised when choosing this treatment route. Implantation is limited to the region of the trachea or main stem bronchi.

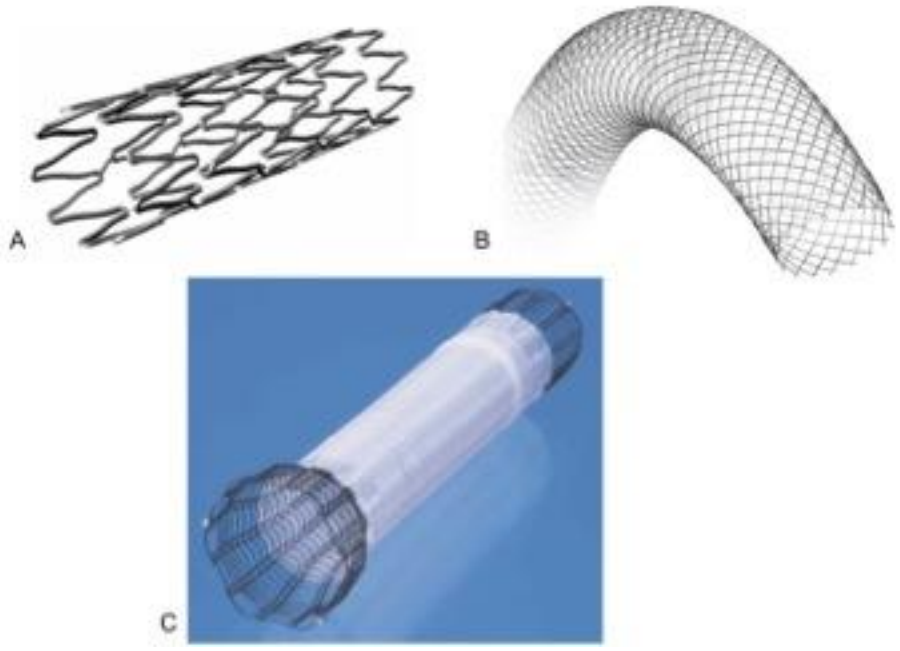

Figure 1.4. Metal stents used today. Products of Boston Scientific. The Palmaz stent (4a), Wallstent (4b), and Ultraflex Strecker covered stent (4c), are all flexible mesh stents.

The Wallstent (Fig. 1.4) is also a woven metallic mesh, but is coated with a polyurethane layer [14]. This design will not collapse when bent or compressed, making it unique among metallic stents. Resistance to collapse allows for the stent to be used

throughout the trachea and less-uniform regions of the bronchial tree. Like many metallic stents, the Wallstent shares a similar problem of causing granulation tissue formation. As the Wallstent is completely compressed, lengthening occurs, while when partially compressed the stent will shorten. The uncovered edges are slightly pointed, thus any movement against the local mucosa will cause a tissue granulation response.

Another metal stent, the Ultraflex Strecker Stent (Fig 1.4), is better adapted to kinked, irregularly shaped, or particularly smooth airways [9]. The wire filaments, which are knitted to form this stent, are made of Nitinol and allow for epithelialization of the stent such that functioning cilia can exist within the stent. The Ultraflex can be used to treat a broad range of tracheobronchial stenosis, including those caused by tumors, and can be used to seal airway fistulas to the pleural cavity, or to the esophagus. Although the mesh allows for function of the mucociliary escalator within the airway, once again granulation tissue formation is a problem to be considered with this stent, along with tissue growth between the mesh.

A summary of each of these stent types, their material composition and subtypes included, are found in Table 1.1. Additionally, benefits and shortcomings of each stent model are also listed, as well as the manufacturers of each respective stent.

Table 1.1. Summary of current major airways stent types and advantages or disadvantages [10].

Stent Type	Subtypes	Benefits	Disadvantages
Silicone	Montgomery T tube, Dumon[a], Hood[b], Reynders[c], Dynamic, Polyflex[d]	Removable/exchangeable, resist external compression, minimal granulation, inexpensive T stents advantageous for disease with carinal involvement	Requires general anesthesia and rigid bronhoscopy, migrates, adherence of secretions, unfavorable wall to interior diameter ratios, unable to conform to irregular airways, interference with mucociliary mechanisms
Balloon-dilated metal stent	Strecker[e],Palmaz[f]	Less migration, thinner so inner diameter is bigger, less interference with cilia	Needs balloon dilation of the stent, rigid bronchoscopy and general anesthesia, difficult to remove, tumor in growth along the length of the stent, radial force may cause necrosis of mucosa and fistula formation. May collapse if external force too great
Self-expanding metal stent	Gianturco Z[g], Ultraflex	Can be placed with flexible bronchoscopy in an outpatient setting, less migration, thinner so inner diameter is bigger, less interference with cilia	Difficult to remove, raidal force may cause necrosis of mucosa and fistula formation, tumor in growth along the length of the stent, may collapse if external force too great
Cover self-expanding metal stent	Ultraflex, Wallstent[h], Alveolus	No tumor in growth along the length of the stent, thinner so inner diameter is bigger, easier than bare metal stents to remove or exchange, less migration, less interference with cilia	Placed with flexible bronchoscopy, radial force may cause necrosis of mucosa and fistula formation, may collapse if external force too great, granulation tissue at ends, may block bronchus

[a]Endoxane, Novatech SA (Grasse, France), [b]Hood Corp (Pembroke, MA), [c]Reynder's Medical Supply (Lennik, Belgium), [d]Dynamic and Polyflex (Rusch, Duluth, GA), [e]Boston Scientific (Natick, MA), [f]Cordis Corp (Miami Labs, FL), [g]William Cook (Bjaeverskov, Denmark), [h]Ultraflex and Wallstent (Boston Scientific, Natick, MA).

1.2.3 Idealized Stent

As mentioned throughout, these existing materials do not satisfy all requirements for an ideal stent, though many are functional and useful tools. Nearly all have reported some form of complications, usually formation of tissue granulation (mainly in metal stents), mucostatis due to necrosis or occlusion of the ciliary system within the airways, and stent migration (particularly in Dumon, Noppen, and Polyflex polymer stents) [9,15,16]. Ideal stent properties have been outlined after multiple experiments by various

authors. These much desired and superlative properties require that stents are limited in the amount of migration, tissue morbidity and mortality, additionally are easily removed and placed, result in minimum granulation tissue formation, and maintain the potency of the laminal tissue which the stents are placed in contact with [10,15] such that the natural mucociliary escalator system in the airways is undamaged. In addition, an economical or cost effective product would also be more hospital, and patient-friendly.

CHAPTER 2. THREE DIMENSIONAL PRINTING AS A SOLUTION: PROMISES AND SHORTCOMINGS

2.1 Tracheobronchial Stents and 3D Printing

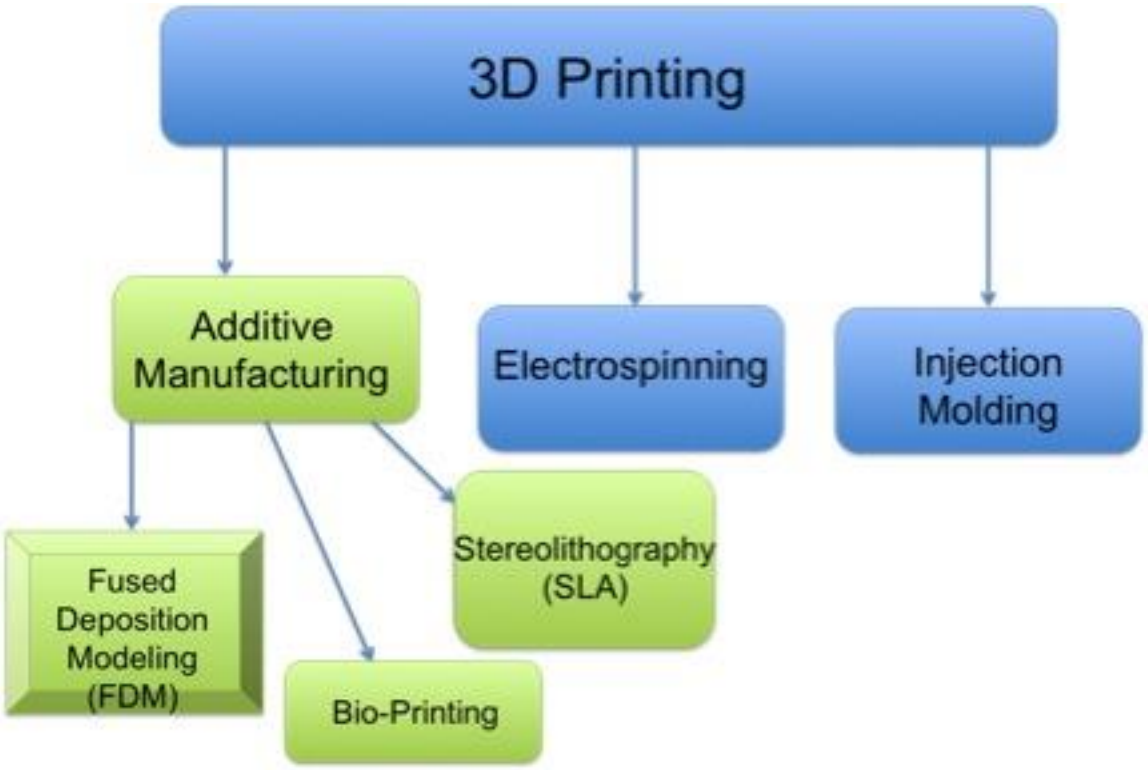

Figure 2.1. A sample of the different types of 3D printing and 3D manufacturing available today. While the fasted growing of the categories is AM, and of that, FDM and Bio-printing, the 'bio-printing' process is still experimental and under development.

In this research, FDM (Fig. 2.1) printing is the primary method employed for biodegradable/biocompatible stent design. Among its many benefits is the advantageous feature of obtaining a device directly from the input 3D design within a matter of hours, which makes it the most established and practical additive manufacturing (AM) method in the medical field today [17, 18].

Creation of a three-dimensional stent requires specialized equipment. While an idealized stent needs to fit certain biological parameters and a set of engineering parameters to make such a stent possible, economical parameters such as cost-effectiveness are equally crucial. Depending on the material state, the stent is three-dimensionally manufactured using a particular specialized process. For liquid-state materials, such as liquefied metal alloys, stereolithography (SLA) is employed. For solid materials in filament form, fused deposition modeling (FDM) is used. In this research we focused on fused deposition modeling printing. Among its many benefits, FDM printing allows manufacturing of stents that are customizable for individual patients; a design aspect in much demand in the medical sector. With rapid advancements in this 3D printing field married to medicine, pioneering the creation of the ideal stent can be that much closer at hand.

2.1.1 Techniques of 3D Printing

Various methods of manufacturing stents are used today (Fig. 2.1), and all of these methods are regarded as “three-dimensional” (3D) printing. However each method has advantages and disadvantages. In this section, we describe the various 3D printing methods. For tracheobronchial stents, the method of manufacture depends heavily on the material.

Metallic stents are traditionally manufactured with subtractive manufacturing, in which a laser cuts a piece of metal according to input parameters from a computer aided design (CAD) type software to create a special netted wire mesh; 3D printing methods for metal stent manufacturing involve selective laser sintering (SLS), in which metal or metal

alloy powders are partially melted locally in order to conglomerate and form a solid netted stent layer by layer [19-22]. Once cut, the stent is then prepared for coating using techniques like chemical finishing and laser deburring. The stent can then be coated via electroplating, or simply undergo electro-polishing. These processes are undertaken in order to improve biocompatibility or to bestow biologically inert characteristics to the stent [19, 20].

Metal injection molding is a method in which liquefied metal is forced through a mold to create the final product geometry [21]. Assembly of wire filaments is a method in which metal or metal alloys are made into filaments and assembled into a final mesh design. These are alternative methods that can be employed when manufacturing a metal stent, but depend on the metallic stent design in question [19].

Injection molding methods are primarily used for silicone polymer stent manufacturing. Formation of the mold, however, must be completely personalized to the patient, leading to great expense and time-consumption to achieve the final cured geometry [23]. Because of this, many of the silicone stents available on the market today are simply tubular structures, similar to the 'gold standard' Dumon stent (Fig. 1.2).

While customization of a mold is time consuming from a manufacturing standpoint, customization of products is the ideal standard for reducing overall cost and care-time in the health sector, particularly from the standpoint of the patient and of healthcare companies. For this type of personalized manufacturing (that is, for stents made of metal and silicone), additive manufacturing (AM) is the de facto method [24-27]. AM is the fastest growing printing method, particularly in the medical sector [18]; this is due to AM's capability to produce small-scale tools or products with a berth of detail.

AM can make use of three types of materials, using different specialized sub-techniques for building with each material. As aforementioned, SLS manufacturing, a type of AM, is used for solid materials, but specifically metal; for polymer resins in liquid form, stereolithography (SLA) is preferred, although metal powders can also be combined with liquid polymer to create a finished metal part [73]; both powders and pellets are made into filaments for which fused deposition modeling (FDM) is the method of choice, both of these also being AM subtypes.

2.2 Materials for Printable Stents

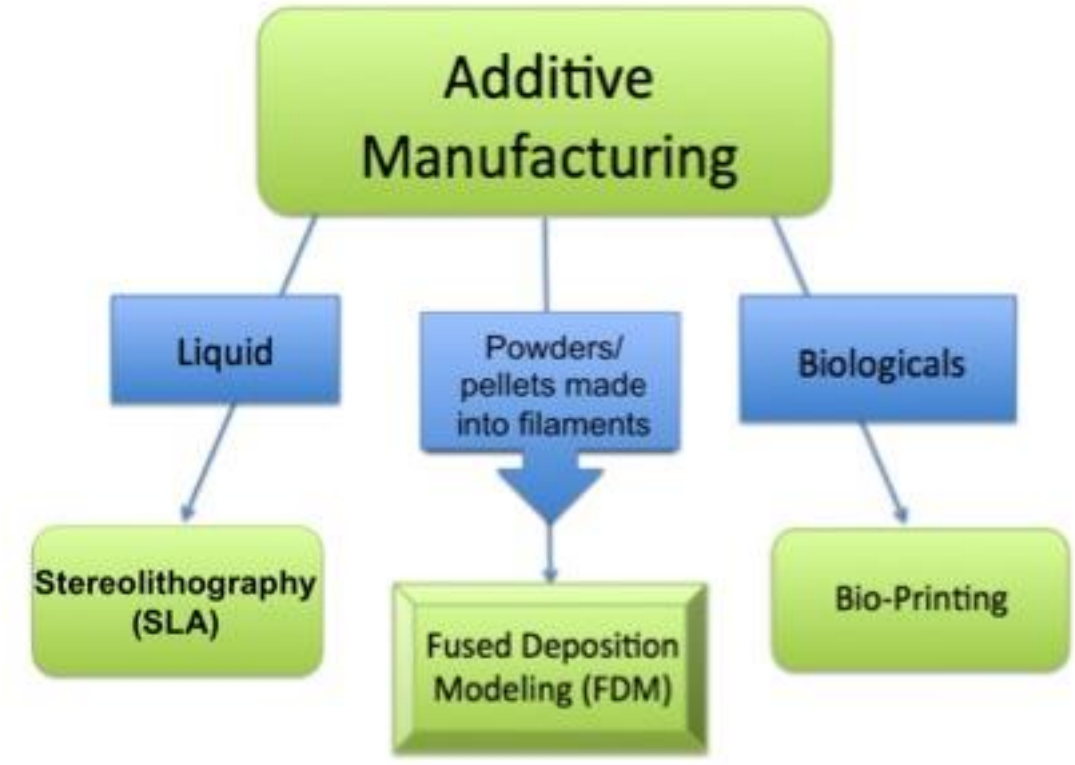

Figure 2.2. Examples of forms of additive manufacturing which are specialized for particular material types. Metals and metal-alloys are used in powder form and are processed using SLS printing; many polymers and ceramics come in powder form, although polymer resins are also available for SLA printing methods. Polymers are also found in filament form and available as spools. Biologicals involve introduction of live cells to print tissue, but this is done by first printing a scaffold and later introducing cells into the scaffold to create grafts, etc. As of yet there are no printers that can directly print living, wholly undamaged cells.

All material considerations for stents in this research were required to be either bioresorbable, biodegradable, or biocompatible; therefore these key terms must be clarified for the reader. The generally accepted definitions are as follows.

Materials that are 'bioresorbable' are completely eliminated from the body via natural pathways like metabolizing or filtration of the byproducts, after bulk degradation of that material [28, 29].

'Biodegradable' materials are defined as solid materials (including gels, grafts, and implants), often of polymeric nature, that undergo macromolecular degradation *in vivo*. This breakdown results in byproducts or fragments that do not necessarily exit the body, but are removed from the site of action [28, 29].

While there is a broader definition for those materials termed 'biocompatible', the FDA and European Society for Biomaterials (ESB) accepted definition of a medical device that is biocompatible states the material should not elicit any undesirable systemic or local effects, (such as toxicity or carcinogenic effects) [30, 31]. It is further stated that the biocompatible material should elicit an 'appropriate and beneficial' cellular or tissue response for that given situation.

Existing stents tend not to be biocompatible, but rather are biologically inert at best, and employ a limited set of material types, namely silicone, metal-alloys such as Nitinol, other metals such as Teflon [32, 33] or stainless steel [34], or a combination of any of the aforementioned elements. In order to more closely achieve an idealized stent, other materials with better biocompatibility are a necessity. Material science has grown in leaps and bounds, producing many polymers with biomimicry capabilities, or substances that can harmlessly breakdown over a determined amount of time and are then flushed

from the body via the usual rheological route. Elements native to the body have also been aggressively studied and put to novel uses while maintaining the natural properties that they are biologically specialized for.

In this research, we are focusing on FDM, which has certain material requirements. Three types of materials were investigated for this research—ranging from most natural and biodegradable, to least natural but biologically compatible. The first, collagen type I, is a native, biological material; the second, middle-spectrum material, polycaprolactone, is highly biocompatible and biodegradable but is also a synthetic/soft-biopolymer; the third, thermoplastic polyurethane (TPU), is a promising biocompatible polymer. These materials have yet to be tested for stenting, or yet to be proven as manufacturable through the novel methods of FDM printing to create functional tracheobronchial stents.

Collagen is the most natural of the materials we investigated; it is also the most abundant in the mammalian body, making up 25-35% of the body's total protein content [35, 36]. This material is type I "fibrillar protein" collagen. On the nano-scale with its highly organized alpha helices base, throughout till the micro-level with its intricately structured fiber bundles, the architecture of collagen type I boasts high tensile strength [37-40]. Viscoelastic properties of collagen, particularly as a hydrogel [41, 42], also favor the use of type I collagen as a biomaterial for stent making. Additionally, cells easily attach to and degrade collagen, allowing for reintegration of living tissue and production of new collagen intercellularly in areas surrounding the implanted biomaterial [36].

Collagen is optimized for laying the structural foundations for a variety of tissues in the body, making collagen type I conducive to rebuilding a tracheobronchial passage

suffering from symptoms of atresia or malacia. Fibrillar protein collagen is also very versatile; capable of being reconstituted into hydrogels, macro-scale constructs such as tissue grafts, microspheres for drug-delivery, or cell-seeded scaffolds, all of virtually any shape and size [36].

While type I collagen holds much promise, few documented attempts have been successfully made in creating a mostly- or fully-collagenous stent. Of all recorded papers, the closest few, as of today, include an artificial tracheal collagen-coated mesh prosthesis which was attempted as a basis for wound healing [33], with a similar type collagen-coating attempted for a drug-eluting vascular stent [43]; an experimental carinal reconstructive prosthesis conjugated with collagen coating was documented [44], and a PLGA-collagen hybrid scaffold, reinforced with a copolymer stent and hydrogel, was more recently attempted as a means of tracheal defect repair [45]. All these attempts had relative success, underscoring the potential of collagen as a viable biomaterial for tracheobronchial stent design.

With the aid of novel manufacturing methods such as 3D printing, in combination with advancements in today's technological equipment, this research could successfully lay the groundwork for a type I collagen, resorbable tracheobronchial stent.

While materials, like type I collagen, which are inherently found in the body may hold the best solution for compatibility and eventual reintegration of stents for long-term recovery, materials that are highly biocompatible and/or bioresorbable are also very promising. Among these is polycaprolactone (PCL), a semi-crystalline aliphatic biopolymer that has biodegradable and biocompatible traits [46, 47, 48]. Unlike fibrillar protein collagen, PCL's surface hydrophobicity, while good for slowing its degradation

rate, undermines its effectiveness in allowing cell adhesion and eventual reintegration into local tissue [49, 50, 51]. However, PCL can be broken down by microorganisms outside the body quickly, while within the body it is slowly resorbed after the initial hydrolysis-based degradation takes place [52]. Surface erosion, or degradation, occurs when the surface-level polymer backbone is being cleaved hydrolytically, resulting in external polymeric thinning while internally the molecular weight is basically unaffected and will remain unchanged while degradation occurs [53]. With erosion of the polymer occurring in this fashion, the lifetime of the breakdown process can easily be predicted, and release rates for drug eluting implants and similar medical devices are readily calculable [54]. This feature gives PCL the 'bioresorbable' property that has made it popular for implants and tissue engineering scaffolds, sutures, wound dressings, and dental devices, among many other medical uses [29].

Materials that are deemed bioresorbable tend to double as being biocompatible, given that the body's tissues tolerate that same material well [55]. Being both biocompatible and bioresorbable, PCL has ideal rheological properties and can easily exit the body harmlessly, while its viscoelastic properties mean production and manipulation of the polymer are easy, and degradation time can be specifically tailored to fit the particular, necessary device lifetime [29, 54]. Because of its many favorable traits, attempts have been made to use PCL to fabricate a tracheobronchial stent for airway remodeling in the past [56, 57]. None of these attempts thus far employed novel 3D printing methods, or have proven that this material is 3D printing-compatible.

The third material studied in this research, TPU, is biologically compatible [58] rather than bioresorbable, and has potential for stent making. The mechanical properties

of this thermoplastic polyurethane (TPU) compound would make the printing of a great variety of personalized stents easily plausible. TPU has high strain recovery and is highly tunable or “smart”, meaning it will return to its initial shape; it is light weight and easy to process, making it ideal for 3D printing, in addition to being low cost, which makes it economical [59, 60].

FDM methods like 3D printing require filamentous material input; the heat-based extrusion process has the potential to alter material properties, particularly of thermoplastic or thermally sensitive substances like TPU. Extruded TPU under repeat cyclic-loading and unloading, which are conditions an implanted stent is likely to experience during reflexive events such as coughing, eventually exhibit inelastic effects such as residual strain, hysteresis loss, and stress-softening; this is usually under maximal strain, however [61]. Given thermoplastic polymers have high resilience and low stiffness, while handling friction well [62], and because these polymers have shown higher strain capability and strain recovery values when copolymeric sequences are more randomly distributed [63], the aforementioned problem of inelastic/plastic deformation can be worked around.

An additional concern for thermoplastic composites in general includes the plasticizing effect which moisture absorption has on the material [64, 65]. Medical grade thermoplastic polyurethanes have been used in completely moist of fully humid environments such as the mouth or intravenously, either for orthodontic purposes or vascular grafts, respectively [63, 66]. Based on this information, it can be deduced that if TPU can successfully be cross-linked in a manner that creates material insolubility, it is possible to employ this biomaterial for tracheobronchial stent printing. While this

material has been used in combination with 3D printing in the past, there is no documented use of TPU in tracheobronchial stent design as of today.

2.3 Stent Printing Process

For this research, FDM printing is the primary method employed for biodegradable/biocompatible stent design, given the advantageous feature of obtaining a device directly from the input 3D design, which makes it the most-established AM method in the medical field today [17, 18]. FDM traditionally only makes use of the filament-form of any material; that substance is then directly deposited using a system of layers building upon earlier layers, until the final device is formed. Silicone stents have been manufacturing using a very similar technique, but often must be injection molded and require a lengthy curing process afterward [67, 68, 69]. TPU polymers are flexible and share many mechanical properties which are similar to the traditionally used silicone, but TPUs are designed to be more 3D printing friendly, while polymers like PCL, or biological materials like type I collagen, have not been successfully printed using FDM technology; attempting this pioneering process with these materials is also part of the focus of this research.

As newly available biological materials that increasingly emulate natural tissues are becoming widely accepted for use in the medical field, these materials show great promise for the future of endoprosthesis [70]. In combination with an innovative stent design and manufacturing technique, the creation of a prototype stent not made of silicone or metal, but with materials of ideal mechanical properties like thermoplastic polyurethanes (TPU) [59, 60, 58], high biocompatibility like polycaprolactone (PCL) [29,

57, 71], as well as a biomaterial like fibrillar protein collagen with potential for resorption into the airway [36], would provide a novel, unique edge to research at the University of South Carolina.

CHAPTER 3. STENT TESTING

3.1 FDA Non-Clinical Evaluation Requirements

The FDA requires certain mechanical properties be quantified for non-clinical evaluation of stents [72]. However, no widely accepted, industry-standard protocol exists for obtaining these properties for airway stents. The FDA publishes specific guidelines for vascular stents that can be adapted for airway stents. For this research we performed certain basic mechanical analyses, such as tensile testing and compression testing, to characterize both the raw materials for each of the stents proposed, as well as the post-processed form (stent) itself. The significance of these properties to airway stent performance will be described in this section.

After a stent is designed, documented testing is necessary in order to demonstrate safety and proper functionality in accordance with FDA guidelines. This allows physicians to determine under what conditions, and where, the best stent placement should be.

While no particular FDA protocols are given for airway stents, there are certain mandatory, non-clinical engineering data or properties that the FDA requires be quantified. Among these requirements are forms of uniaxial compression or elongation (extension) testing (Fig. 3.1), to characterize a stent's performance under short and long-term external loading/unloading [72]. Stent stress and strain responses determine stent strength. Specifying the plasticizing point (the point of irreversible deformation known as

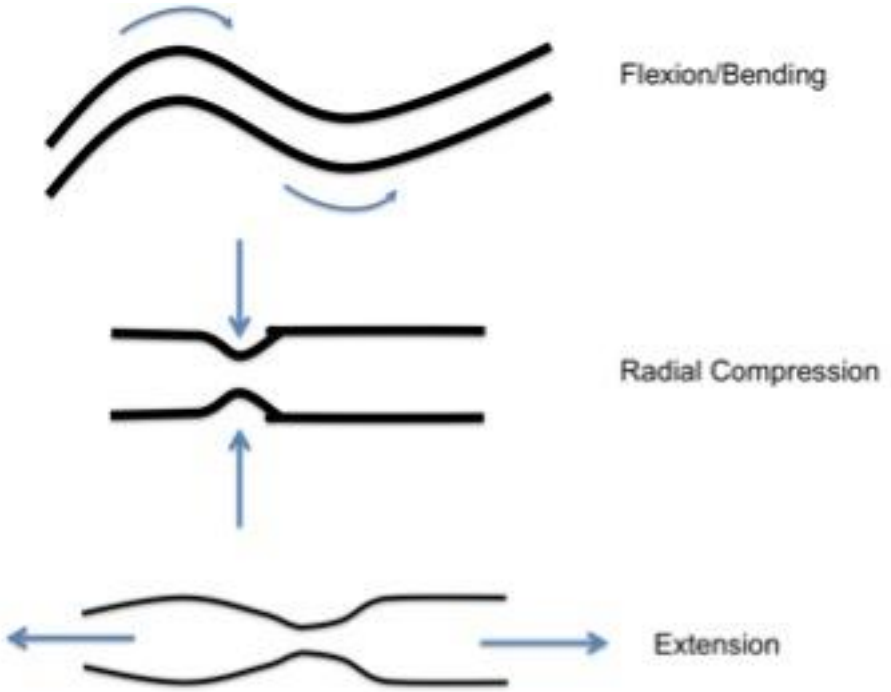

Figure 3.1. Some stent characterization tests. Angles of forces applied to stents during various standard tests that will determine maximal stress or strain the stent can withstand.

yield strength), and its maximal deformation limit, (known as the ultimate tensile strength point) for each stent will directly correlate with its clinical performance.

For certain stent designs, for example mesh stents and expanding stents, the FDA also requires particular radial strength and radial stiffness testing unique to each stent's specific dimensions. Material composition also requires certain additional tests for yield strength, elastic (Young's) modulus, and endurance limit, among others [72]. Again, these quantify the strength of the stent.

3.2 Expandable or Self-expanding vs. Solid Stents

The stents manufactured in this research are all termed 'solid' stents, having the straight-tube design similar to the industry gold standard Dumon stent. Solid stents are

delivered using rigid bronchoscopy, and are already in the final conformation state they have while deployed within the trachea or bronchi; therefore these are not considered 'expandable' stents.

In contrast, an expandable stent changes shape after insertion. Expandable stents are further divided into either balloon-expandable or self-expanding stents. Balloon-expandable stents are usually delivered via the flexible bronchoscopy method (this procedure does not require general anesthesia), and as the name implies, such stents are maneuvered into place prior to being expanded to their final conformation. Stents of this type are usually tightly wound over a flexible catheter tipped with a small balloon (Fig. 3.2), which is used to guide the stent into place, then inflated by the physician in order to deliver the stent. The balloon is deflated once the stent is placed, and the catheter itself is removed.

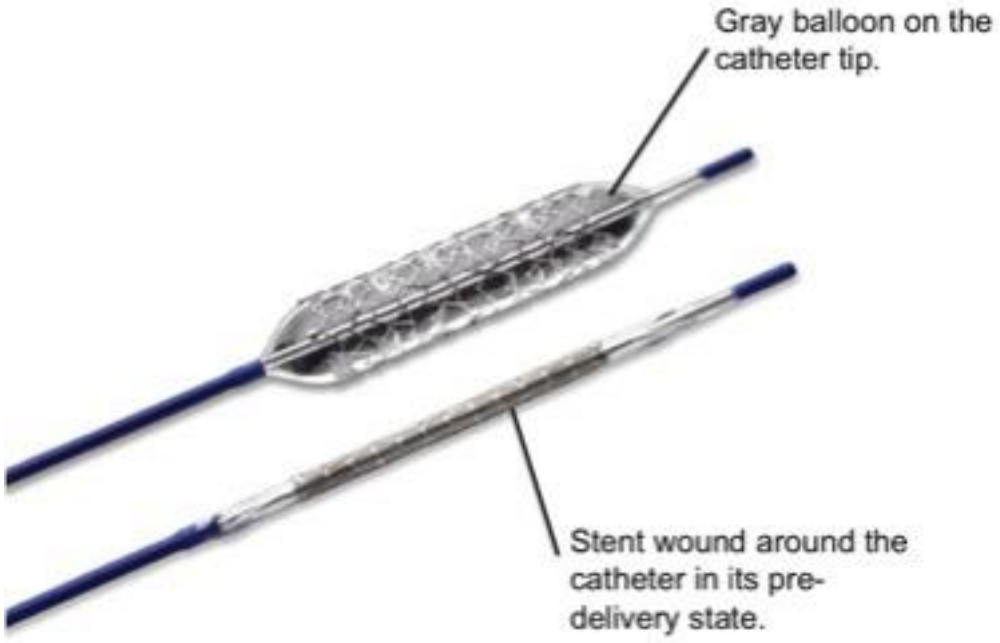

Figure 3.2. Balloon-expandable stent. Mounted on a flexible catheter and delivered to the deployment site, prior to balloon expansion. Once the stent is placed, the balloon is deflated and the catheter is removed, leaving the stent in place. Above delivery system is produced by Covidien.

Self-expanding stents are ‘spring loaded’ into special catheters. Once the catheter is correctly positioned, the stent is released from the device and immediately expands to achieve its final conformation (Fig. 3.3).

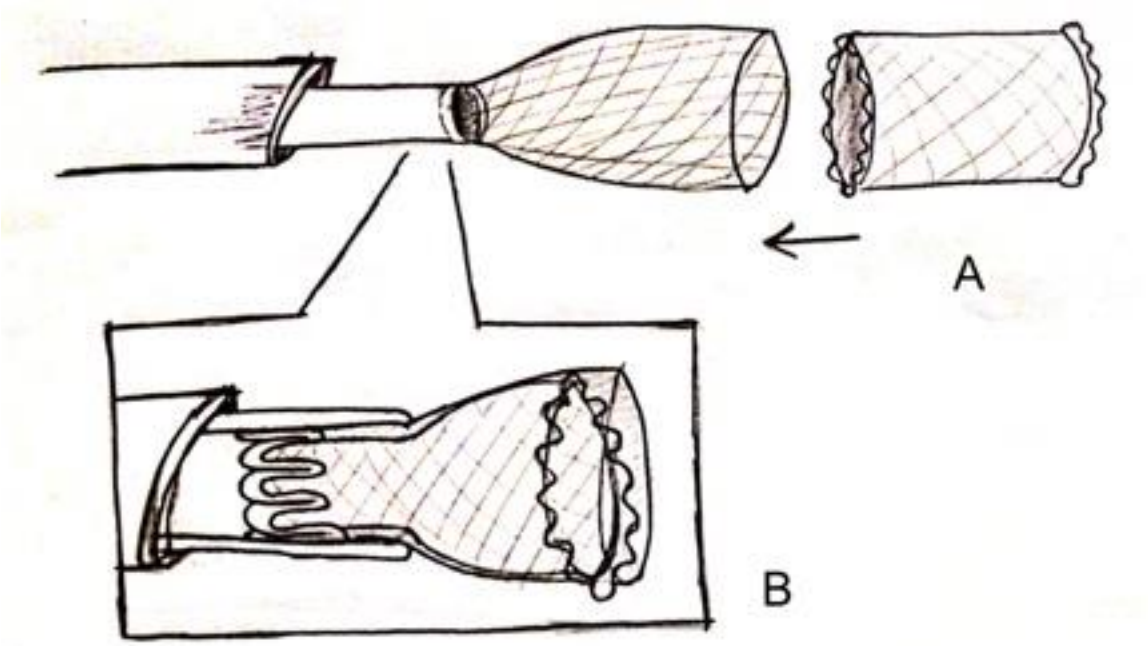

Figure 3.3. Schematic of a self-expanding stent and delivery catheter. In 3.3A, both the loading of the stent into, and the delivery out of, the instrument is facilitated via a netted sleeve. Illustrated in 3.3B, the stent is being compressed as it is loaded into the netted sleeve such that it may deploy and expand to appropriate geometry when delivered into the airway.

Additional properties to report for balloon-expanding and self-expanding stents are required by the FDA to determine the recoil and radial outward force exerted by the stent on the surrounding tissue. Forces that are too great risk a possibility of damaging tissue local to the stent. Weak expansion forces may result in a partially deployed stent, which in turn could occlude the area in which the stent was placed, or cause the stent to migrate out of the target location. Foreshortening, or the potential change in stent dimensions affecting stent length as it is being deployed, must likewise be evaluated [72].

Testing that exceeds FDA requirements has been undertaken in past research to study stent migration and behavior. Such testing includes stent behavior in the tracheal region under conditions of coughing, *in vivo* studies, or development and modeling of stent behavior using complex simulation software [75-77]. Such testing is beyond the scope of this research.

CHAPTER 4. TYPE I COLLAGEN STENT ANALYSIS

4.1 Designing and Manufacturing A Simple Tubular Collagen Stent

One of the goals of this research was to create a simple, smooth-walled stent similar to a basic Dumon silicone tube stent. We created three tubular collagen stent prototypes with the injection-molding 3D printing process. Such stents allow for comparison of the material properties of each the 3D printed stents to the Dumon silicone stent that holds de facto go-to status for non-metallic stents.

While direct FDM printing of gel-like collagen would be most advantageous (see Chapter 2), such is not yet possible. Our procedure was to use SLA methods to print a mold (Figures 4.1-4.3) from an acrylonitrile butadiene styrene (ABS)-like material. This mold was subsequently used for the 3D injection molding of the collagen stent. Injection molding was most conducive to working with raw type I fibrillar collagen. A team member, using a CAD package, designed the individual parts of the 3D printed mold.

The collagen was obtained and prepared from the hide of an 18-month-old bovine steer, provided by Caughman's in Lexington, SC.

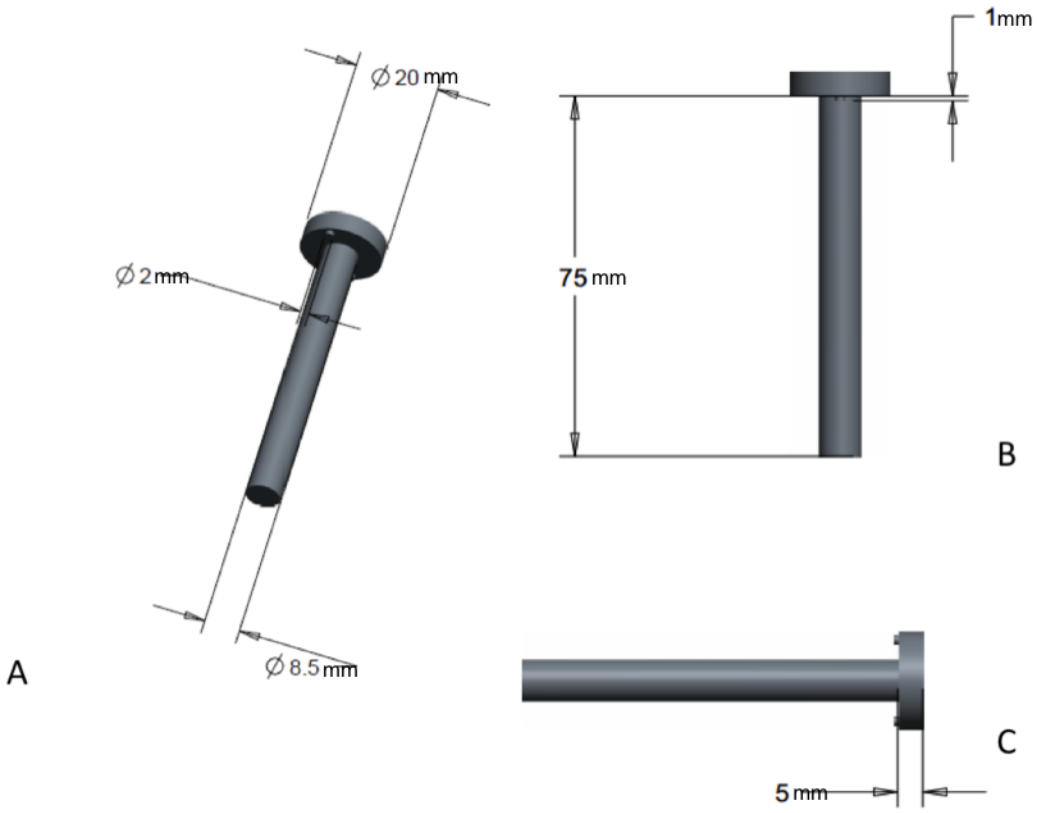

Figure 4.1. Rod designed using CAD software. It is placed in the center of the mold, allowing for construction of patent inner lumen of tube. Various angles are shown here along with respective measurements.

Because collagen was demonstrated to be more conducive to the injection molding 3D printing method than to the FDM method, simple collagen tubes were manufactured via injection molding using standardized methods, and were mechanically tested (Appendix A).

The collagen tubes were already primarily cross-linked via pH crosslinking, in order to set each tube in its respective mold. Next, the tubes were further polymerized using UV cross-linked via a UV Stratalinker 2400 introducing 0.12 millivolts of UV light at a wavelength of 166.7 nm in each burst. Polymerization was done to further increase stiffness to the desired level for testing.

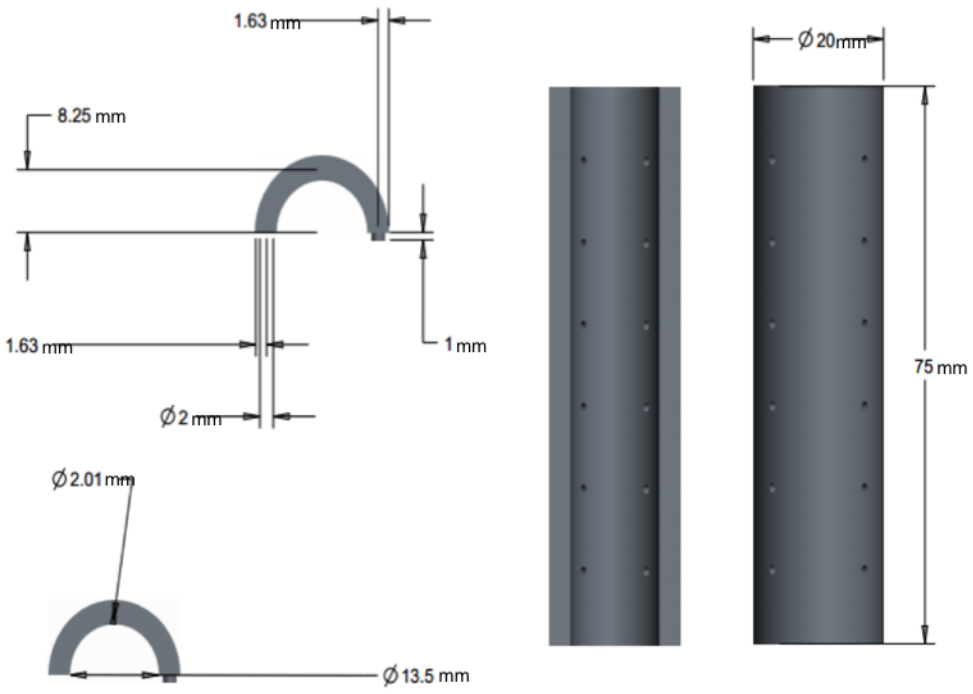

Figure 4.2a. Shell of the mold, designed using CAD software. This design was intended to determine the outer diameter of the tube stent. The pinpoint holes in the body of the shell are in the micrometer range; these are intended to release pressure when collagen is injected in, as the formation of air bubbles compromises stent integrity.

The detailed collagen preparation and concentration procedure is included in Appendix A. Collagen concentration was determined by a weight percent (wt%) calculation:

$$wt\%\ collagen = \frac{Dry\ Collagen}{Wet\ Collagen}\ x\ 100\% \qquad \text{(Eq. 1)}$$

The experimental range of wt% used started with the lowest concentration of 0.5 wt%, the next being 0.77 wt%, another concentration at 0.83 wt%, and the highest concentration being 3 wt%.

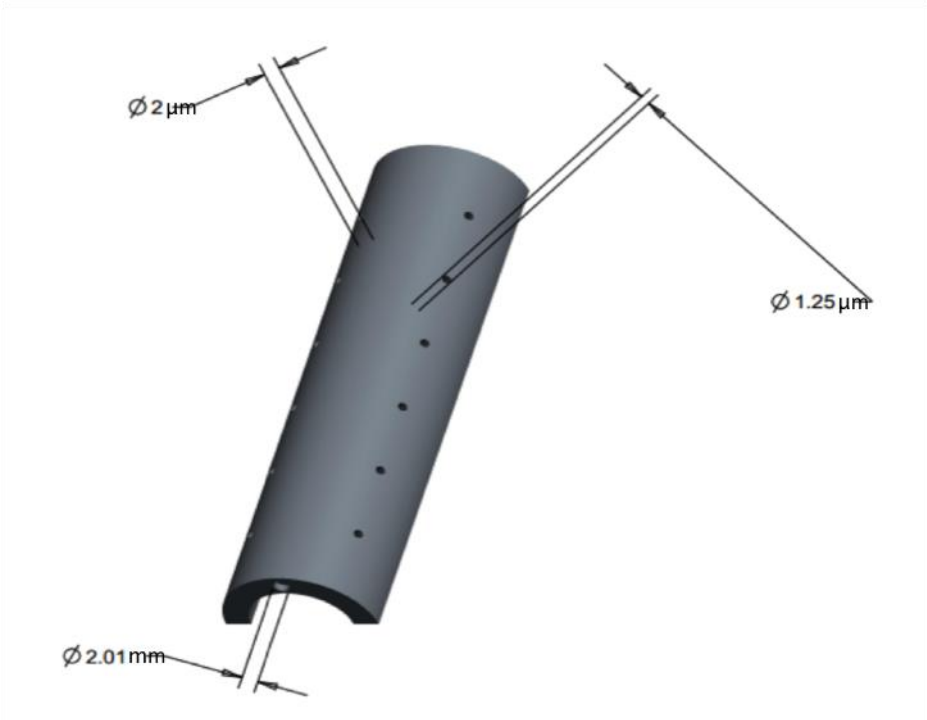

Figure 4.2b. Body of the mold shell. Again, the pinpoint holes of 1.25µm diameter intended to release pressure from injecting fibrillar type I collagen. The 2.01mm indent is where the cap will snap securely into place on either end of the mold shell.

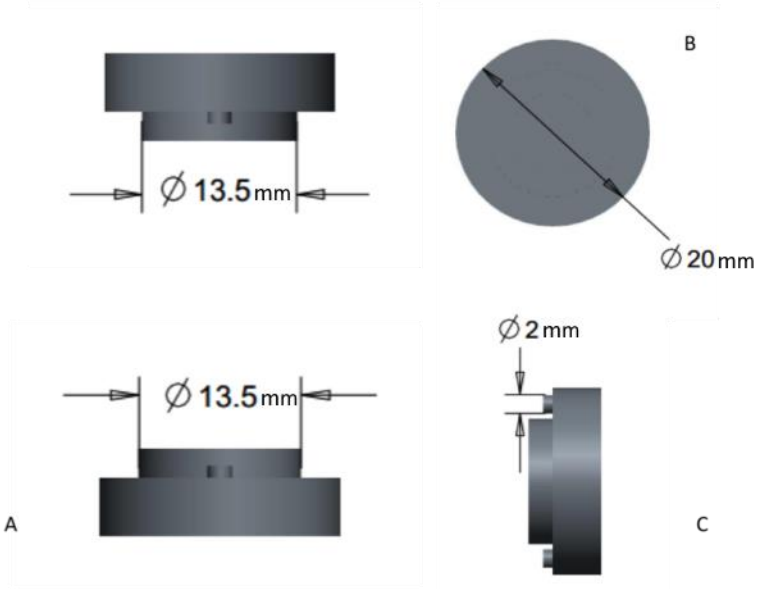

Figure 4.3. Cap of the mold, designed in CAD. Fits on either end of the rod piece, sealing the mold and collagen inside and preparing collagen for pH crosslinking bath.

4.2 Collagen Stent Results

The objective of this research was to use 3D printing methods to manufacture a simple cylindrical tube-like collagen stent and test its mechanical properties. These stress-strain properties were to then be compared to the average total radial pressure force (35kPa) that a tracheomalacial patient's trachea will experience due to flaccid smooth muscle collapse during exhalation. The collagen tubes had a tendency to shrink slightly after removal from the molds and storage in HEPES buffer solution.

Collagen tubes having varying levels of polymerization (0X, 10X, 40X, and 80X) were cut into sections of 2.5mm thick, 7mm diameter discs. Compression testing of the resulting collagen tubes was undertaken using a rheometer. Individual Young's moduli were calculated, along with stress-strain data, and were plotted (Appendix A).

Those collagen discs that were only pH cross-linked enough to maintain their tubular conformation, yet did not experience UV-polymerization (0X cross-linking), were expectedly extremely weak. These discs would deform irreversibly at around 8,500Pa of compressive force. However, the average compressive force experienced by the trachea of a tracheomalacial patient is 35kPa (Appendix A). No significant differences in compressive strength were demonstrated between UV polymerized (10X, 40X, 80X) and un-polymerized (0X) collagen discs of the same wt% collagen. Collagen discs at 3 wt% of all cross-linking levels displayed greater compressive strength compared to those of <1% collagen concentration at all cross-linking levels (Appendix A, Fig. A.15).

CHAPTER 5. POLYCAPROLACTONE STENT ANALYSIS

5.1 Preparing a PCL Filament

Few pure polycaprolactone stents have been manufactured in past studies, particularly for use in the airway; among these few publications, medical grade PCL has primarily been used with other 3D printing methods such as liquid-based SLA or injection molding [56, 57, 74]. Prior to this research, medical grade PCL has not been demonstrated to have been processed into a filament, or, by extension, used in combination with FDM printing.

In accordance with the objectives of this research, the PCL filament was created via the use of an extruder built for this purpose, its optimal FDM printing conditions were determined, and a tubular PCL stent of similar geometry to the Dumon silicone stent was printed. This was then mechanically tested to characterize and compare the PCL stent to the industry standard Dumon silicone stent.

In order to determine if PCL was capable of being FDM printed, and what the temperature specifications of printing were, 12oz of hobbyist quality 'Instamorph moldable plastic' polycaprolactone pellets were purchased from Instamorph [78]. Using a DSM Xplore Micro 5cc Twin Screw Compounder, the Instamorph polycaprolactone pellets were extruded into a 3m long, 1.90mm diameter filament at 90^{o}C, 1.7kN, and 100rpm, with a 1.6mm diameter nozzle tip. The filament was naturally cooled.

On a Solidoodle FDM printer, the Instamorph PCL filament was printed at various temperatures, beginning with its usual melting point at approximately 60^{o}C, until an optimal temperature and maximal speed of printing were determined. Based on this data, we determined that polycaprolactone was FDM printing compatible.

Similarly, 500g of medical-grade polycaprolactone (Mn 80,000) was ordered from Sigma-Aldrich [79] and was processed into a filament using a DSM Xplore Micro 5cc Twin Screw Compounder with similar parameters as above. However, a higher temperature of 93-95^{o}C was required to extrude pellets into the final 1.6mm diameter filament form.

As the Twin Screw Compounder was not optimized for extruding material having the particular viscosity of medical-grade PCL, the Compounder began to singe the PCL filament. Burning results in alterations of the properties of the PCL filaments. In order to prevent introduction of error, an extruder was specially built to process the medical-grade PCL filament. Filament was extruded at 60-65^{o}C.

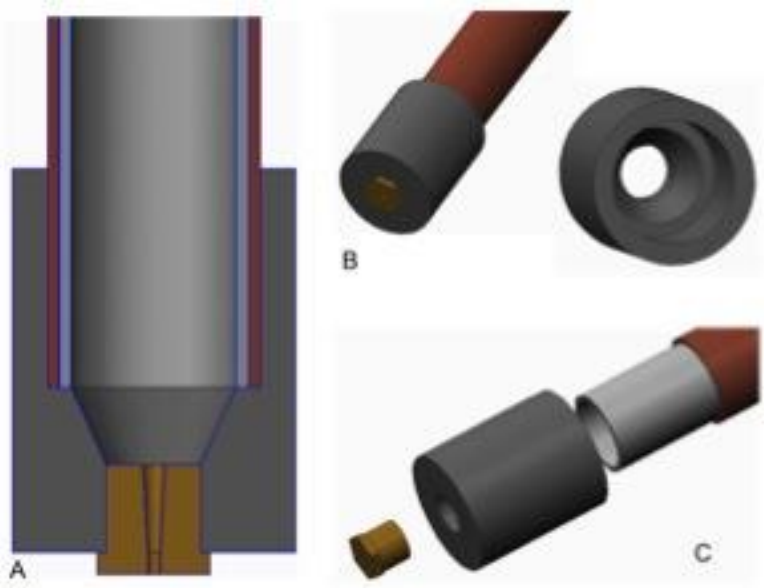

Figure 5.1. PCL filament extruder schematic. Material composition of main body is stainless steel (5.1A, gray and red, 5.1B and C, the red tube); the inner tube is Teflon (5.1A, pale blue, 5.1C, the off white tube) and the nozzle is brass.

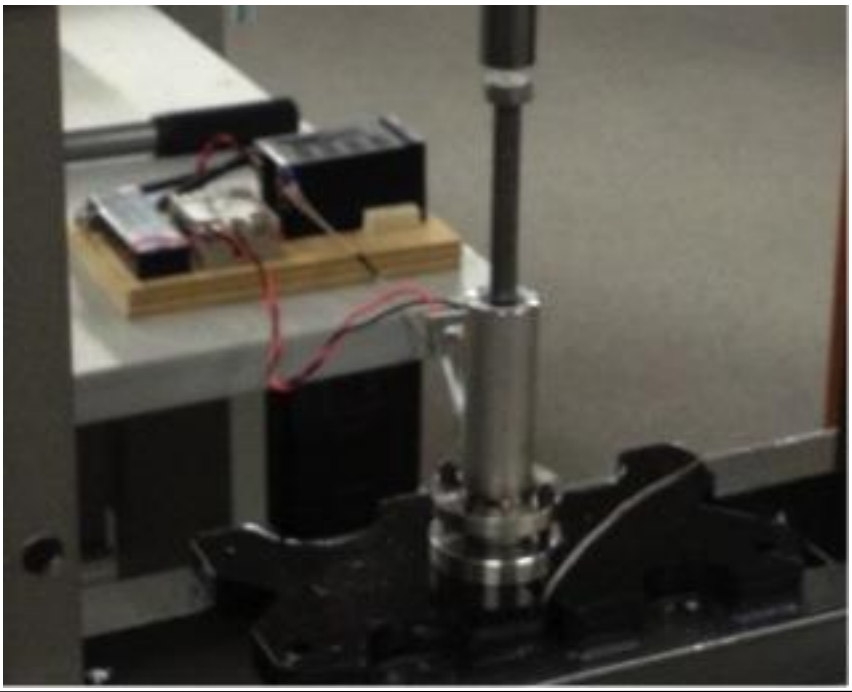

Figure 5.2. Extruder built for manufacturing medical-grade PCL filament. Attached is a thermocouple providing heat for the extrusion process. A team member designed the extruder. The stainless steel extruder body is 13.45cm long with a 33.30mm outer diameter. The opening of the 14.85mm diameter brass tip is 1.58mm diameter. Pellets are poured into 21.55mm inner diameter Teflon body, then the plunger is pushed in using a 12-ton hydraulic shop press.

Tensile testing of extruded medical-grade PCL filaments was undertaken to characterize material properties compared to the medical-grade silicone of the Dumon stent. On a Tinius Olsen 5000, a 1.44mm diameter PCL filament was tested to determine material mechanical properties of stress and strain. The Tinius Olsen 5000 was hooked up to a data acquisitioning device (DAQ) reading voltage output for displacement and force into LabView SignalExpress software. Exported data was then plotted (Fig. 5.3).

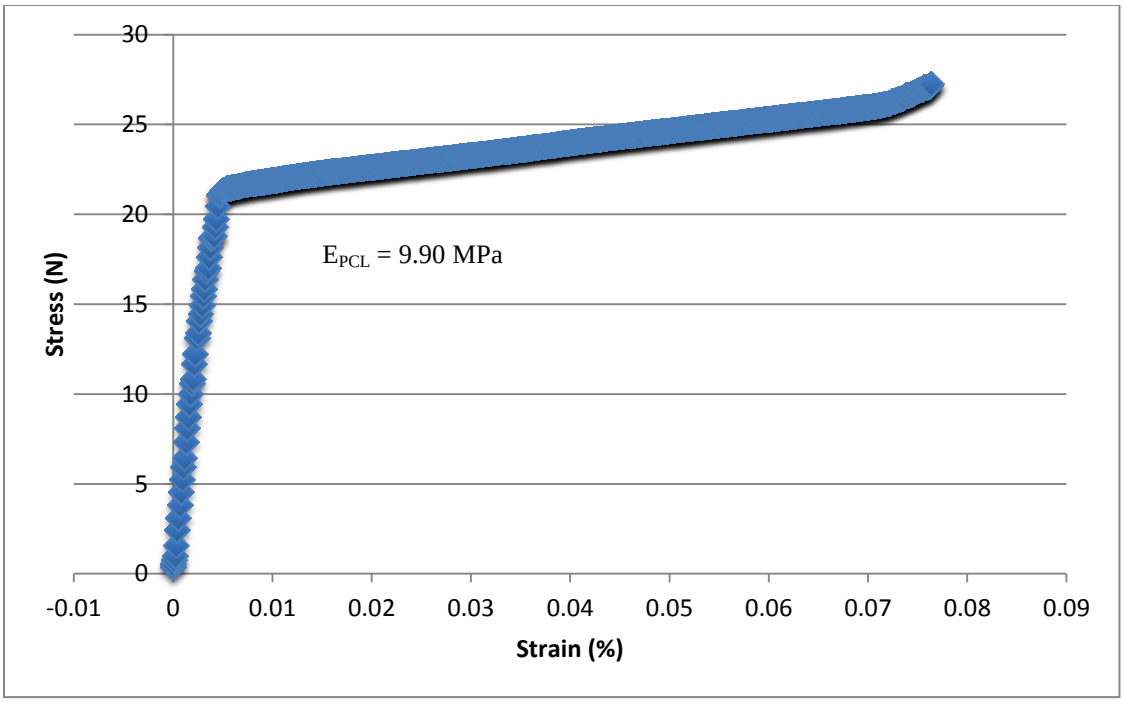

Figure 5.3. Medical-grade PCL filament tensile testing. Average of all trials reported above. PCL filament began necking immediately, but was able to continue to stretch without further decrease in filament diameter for a maximal 12 inches, prior to concluding the test.

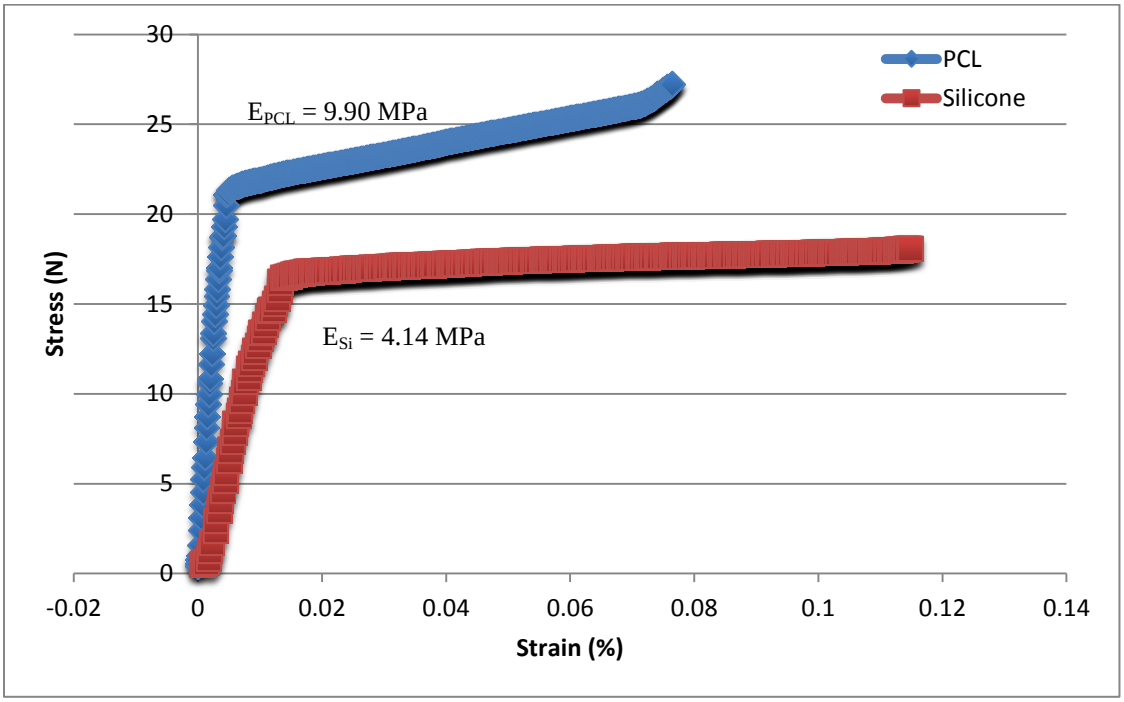

Figure 5.4. Comparison of medical-grade PCL filament vs. medical-grade silicone. A strip of silicone 2 inches long and 5mm in diameter was compared to the 2 inch stretch of 1.44mm diameter PCL. Average trials of both being compared, results suggest that PCL can handle a greater force load compared to silicone for a longer period of time.

5.2 Printing a Simple, Tubular PCL Stent

PCL stents were printed using a Solidoodle FDM printer. The basic schematic is as follows (Fig. 5.2). Filament is fed between the driver and idler gear. Using torque, the gears then feed the filament further into the nozzle where it is then heated; the semi-solid material then exits the nozzle tip to print the final product onto a temperature-controlled stage that can be raised or lowered.

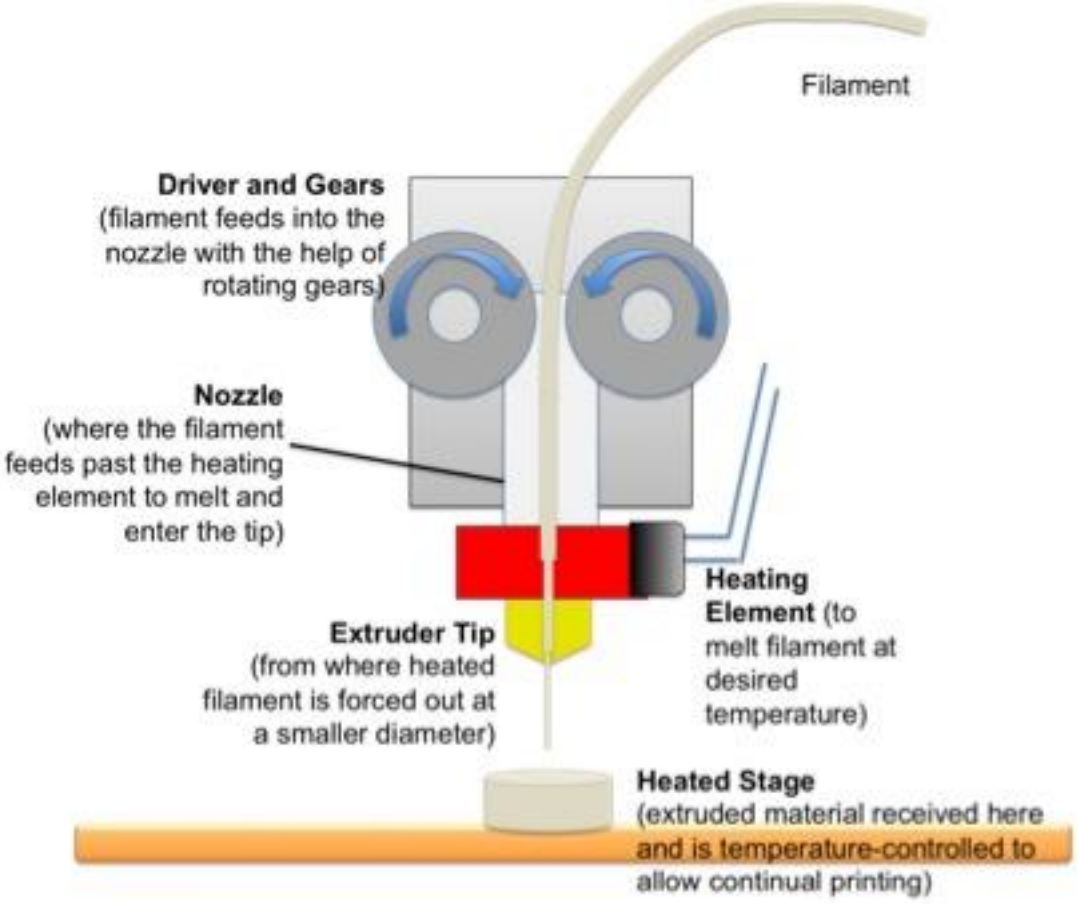

Figure 5.5. Schematic of an FDM printer. The driver motor turns the toothed primary or 'driver' gear, while the secondary smooth 'idler' gear aids in feeding filament into the nozzle. At the end of the nozzle is the heating element that melts the filament, allowing it to be extruded through the tip of the print head and used to print a stent.

Both the Instamorph-grade and medical-grade PCL filaments were printed according to the geometries of the Dumon silicone stent. On a Solidoodle FDM 3D

printer, printability of Instamorph PCL as a biomaterial was tested. At 70^{o}C the filament was extruded consistently at 5 minute printing intervals, supporting that PCL is viable 3D print-capable material.

Similarly, using a Solidoodle FDM printer, higher quality medical-grade PCL filament was printed at 200^{o}C, generating a 30mm diameter ring. Parameters were further adjusted and a prototype simple tubular stent of 7.85 x 10^3 mm^3 material volume was printed in a vertical orientation.

Printed stents were then compression tested using a Bose Electroforce 3200 load frame system (Fig. 5.6), applying 1N of force across the full length of the stent, at a crosshead speed of 0.001m/sec. Compression testing methods used in this research are similar to the previous stent-testing procedures used by Saito et al., 2002 and Liu et al., 2011. The medical-grade PCL stents were compared to industry standard Dumon silicone stents (Fig. 5.7).

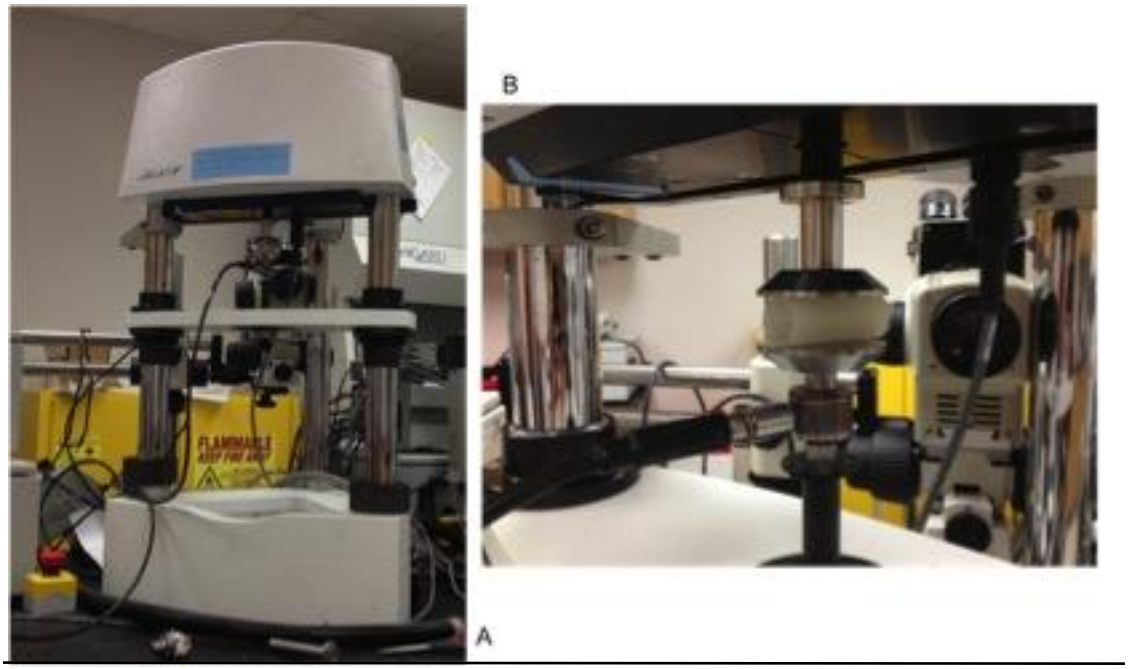

Figure 5.6. Compression testing set up. Using the Bose Electroforce 3200, all stent-types underwent compression testing along the full length of the stent, as in 5.6B, and deformation rates were calculated.

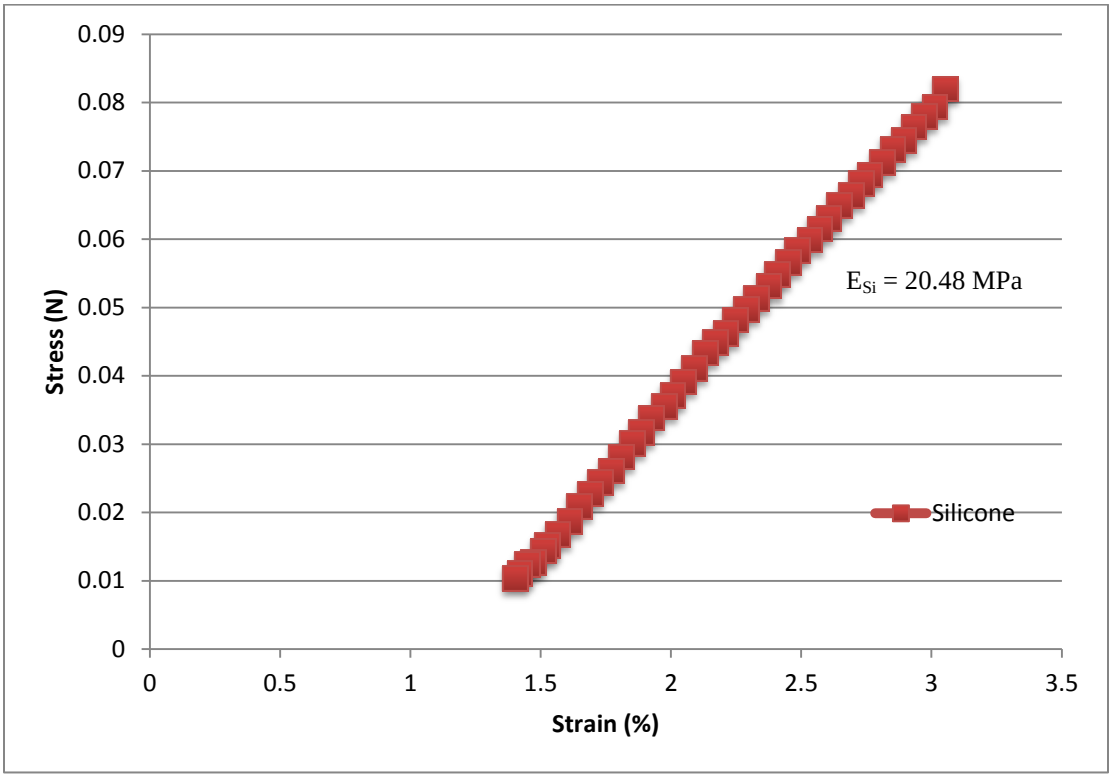

Figure 5.7. Compression testing of PCL and Dumon stents. The PCL stent segment that was compression tested was then normalized along the final length of the final intended stent geometry of both the TPU and Dumon silicone stents. However, the PCL compression testing was not successful.

The final FDM printed PCL stent tested was not the exact length of the testing standard Dumon stent. Therefore, a smaller segment of the PCL stent was compression tested following the above-mentioned procedure for compression testing. The resulting data for the stent segment was then normalized along the final length of a PCL stent that would be geometrically identical to the Dumon stent in length. This normalized data was then compared to silicone compression results.

CHAPTER 6. THERMOPLASTIC POLYURETHANE STENT ANALYSIS

6.1 Printing a Simple, Tubular TPU Stent

A spool of colorless, 1.30mm diameter thermoplastic polyurethane material was purchased from Fenner Drives (trade name 'Ninjaflex') [80]. The material was already in filament form.

Tensile testing of a 1.30mm diameter TPU filament was undertaken using a Tinius Olsen 5000 tensile tester. Force recording was set to 5% force-recording range of the total 5000lb load cell, and extension-recording range was set to a maximum of 25 inches (Fig. 6.1). All data was collected via a DAQ device using LabView SignalExpress software, and exported for processing to Excel (Fig. 6.2).

Figure 6.1. Tensile testing experimental setup using the Tinius Olsen 5000. As in 6.1A, each filament is set in the clamps, exposing a 2 inch stretch of filament for testing. In 6.1B force and extension readouts and parameters are displayed; these remained constant for each raw material test.

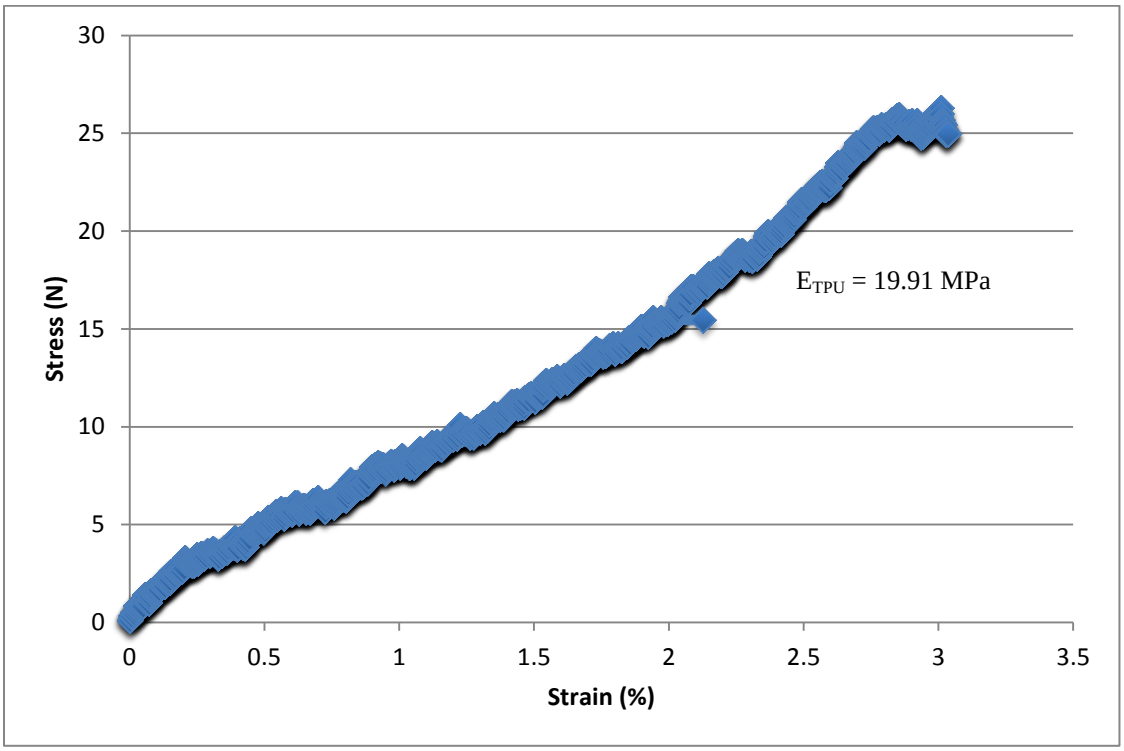

Figure 6.2. 'Ninjaflex' TPU filament tensile testing. Average of all trials reported above. TPU filament was able to elastically recover after each test, returning to its same morphology after undergoing maximal stretching of 10 inches, prior to slipping out of tensile clamps.

On a Solidoodle FDM 3D printer, printability of Ninjaflex thermoplastic polyurethane as a biomaterial was tested. At 205^{o}C the filament was extruded consistently onto a 60^{o}C heated bed. The standard print speed of 30mm/s was maintained. The resulting proto-stent measured 18.61mm diameter x 3mm thick x 30mm length. Evidence supports that TPU is viable 3D print-capable material for the design of implantable airway stents.

Resulting TPU stents were then compression tested using a Bose Electroforce 3200 load frame system (Fig. 5.6), applying 1N of force across the full length of the stent, at a crosshead speed of 0.001m/sec. Stress-strain curves as well as percent displacement were determined (Figures 6.3 and 6.4). Compression testing methods

used in this research are in accordance with previous stent-testing procedures used by Saito et al., 2002 and Liu et al., 2011.

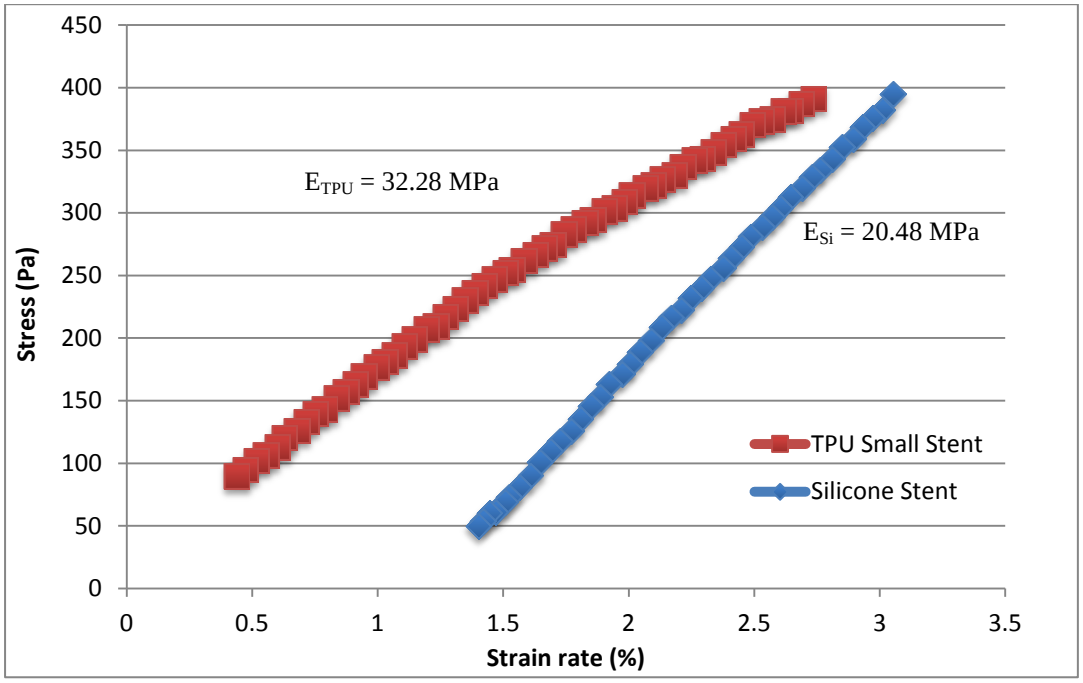

Figure 6.3. Compression testing of printed TPU stents vs. Dumon silicone stent. The smaller diameter TPU stent's radial stiffness ran nearly identical to the silicone stent of the same geometry.

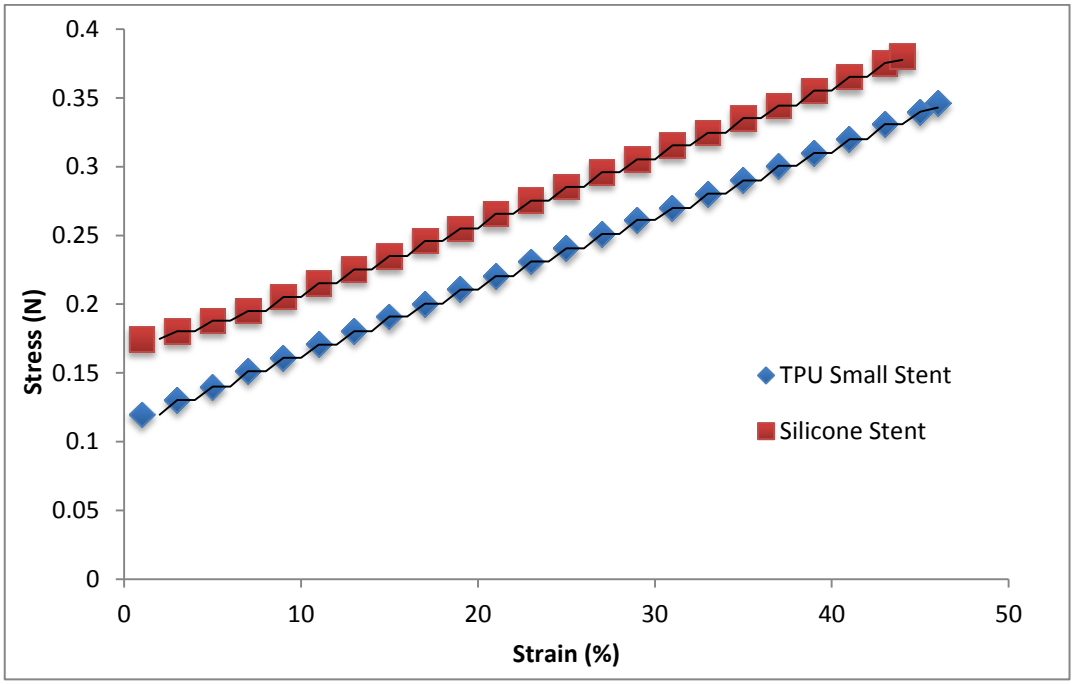

Figure 6.4. Comparison of linearized sections of compression data from silicone and TPU stents. This graph more obviously displays the smaller diameter TPU stent's radial stiffness ran nearly identical to the silicone stent of the same geometry.

All polymer stent tensile (Fig. 6.5) and compression (Fig. 6.6) testing results were compared and plotted. The elastic moduli (E) were also calculated and compared in Table 6.1. It was noted that TPU was capable of further displacement during tensile testing, however, extension beyond the 12in displacement maximum was disregarded as being beyond the scope of research parameters.

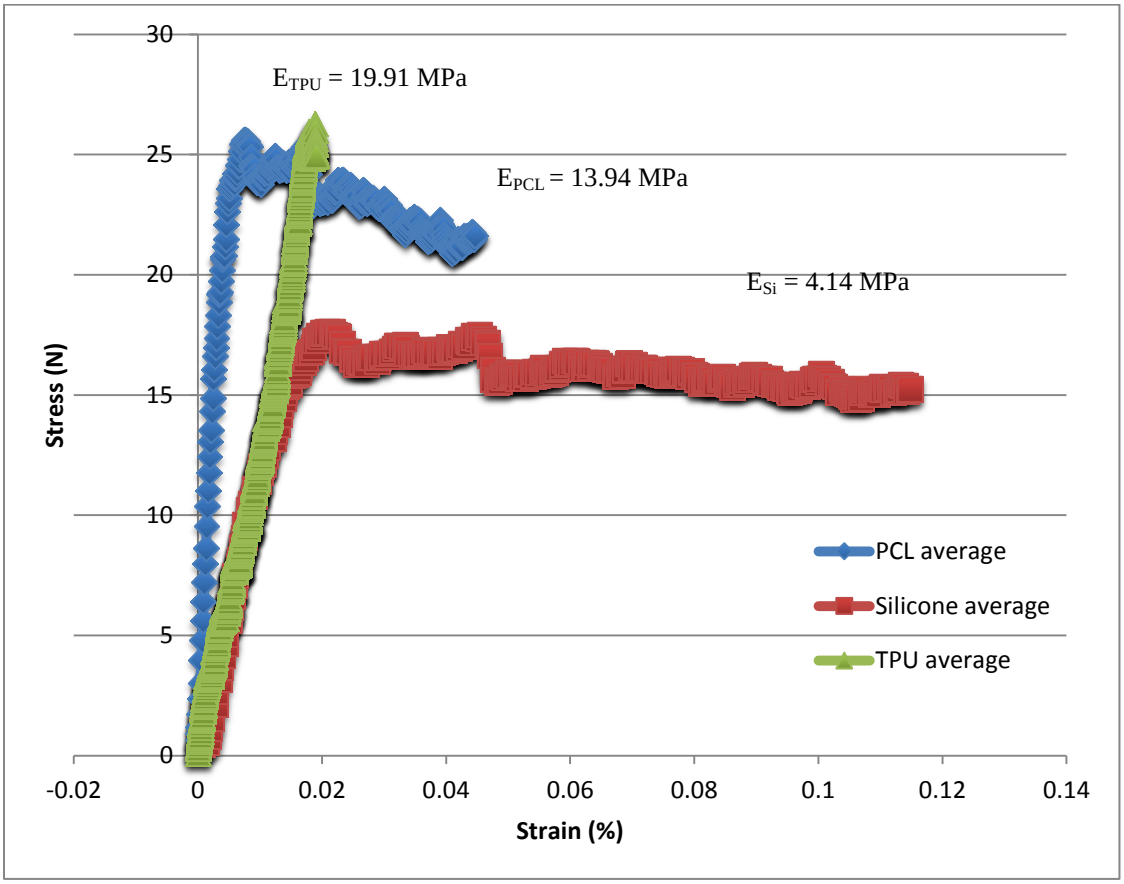

Figure 6.5. Raw material comparison of PCL, TPU, and silicone. Each filament's average is plotted above. While PCL underwent immediate necking, then maintained load bearing steadily, TPU continued to elastically deform. Silicone immediately reached maximal load bearing ability, then maintained its load for a brief period, prior to slipping from the testing clamps.

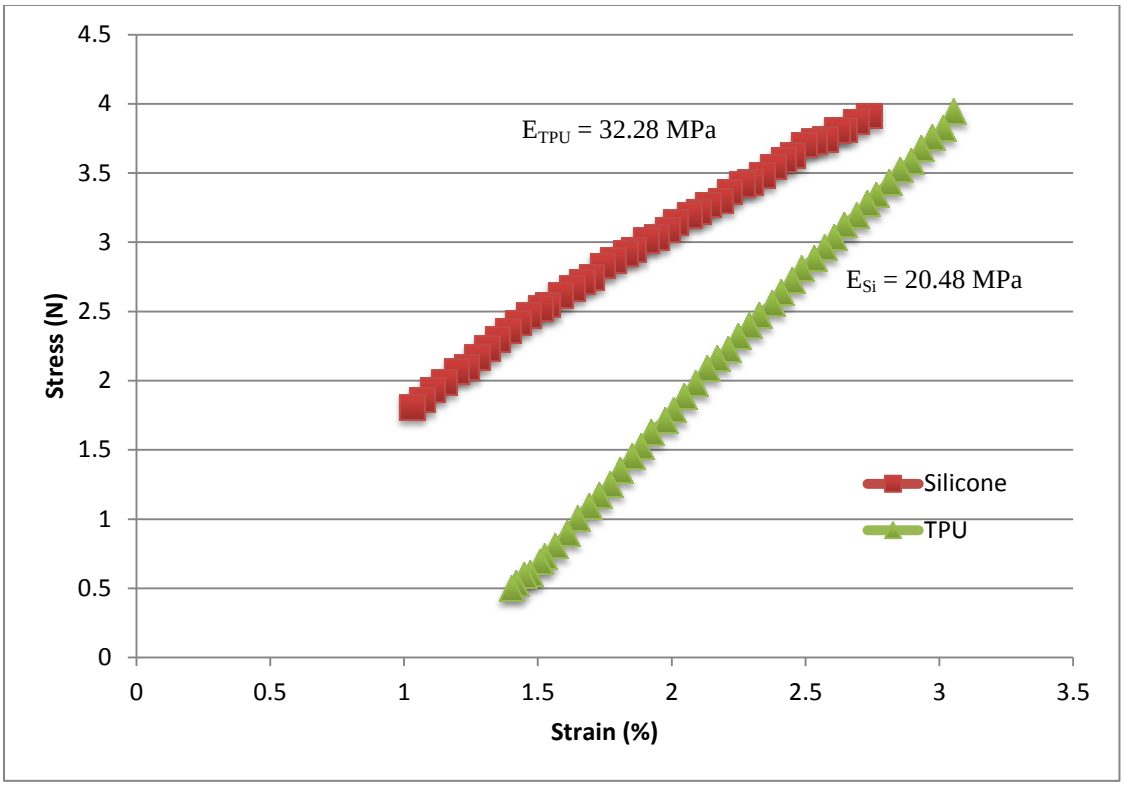

Figure 6.6. Stent compression comparison. PCL, while having a higher elastic modulus than Silicone or TPU, lacked the stiffness of the other stent materials of identical size. PCL compression test failure meant the data was not included.

Testing parameters and results are supported by previously published results for elastic moduli of silicone, PCL, and TPU materials. The general acceptable range for silicone modulus is between 2-6MPa [82], although up to 10-15MPa is not uncommon for medical grade silicone, particularly for airway stents [19, 83]. The general elastic modulus for medical grade PCL (M_n 80,000) is approximately 14-16.9MPa, although changes in polymer chain microstructure can affect this [84]. For TPU, the modulus range begins at 10MPa and goes up to approximately 5GPa, depending on the specific purpose for TPU [85].

Elastic modulus values for a standard tubular stent made from each respective material differ from the raw material values. Unfortunately, the specific elastic

modulus for the Dumon silicone stent was not available for comparison to measured values during compression testing, due to the proprietary nature of the product specifications. While for medical applications acceptable silicone elastic moduli vary anywhere from 3-30MPa [86], and stent elastic moduli must be at least 15MPa for pulmonoscopic insertion [87], the silicone stent tested had an average elastic modulus of 20.48MPa. A PCL stent modulus value can be as high as 352MPa depending on processing method [88, 89], though no standardized value for a pure PCL tube stent has yet been published. Compression results were unsuccessful so the elastic modulus was not determined. For the TPU stent, an elastic modulus of 32.28MPa resulted.

Table 6.1. Comparison of material elastic moduli measured, and respective industry standards.

Material	Elastic Modulus (MPa)
Silicone Strip	4.14
Silicone stent (Dumon)	20.48*
PCL filament	13.94
PCL stent	--
TPU filament	19.91
TPU stent	32.28

where (*) represents unavailable data due to intellectual property.

Again, the geometry of both TPU and PCL stents were identical to the Dumon silicone stent tested, with the exception that the shorter PCL stent segment was tested and data normalized along final stent length to match the Dumon and TPU stents.

Elastic modulus data for raw material and each FDM printed stent are verified by existing publications [84-86, 88, 89], suggesting values for compression and tensile testing align with acceptable stent properties.

CHAPTER 7. SUMMARY AND CONCLUSIONS

Tracheomalacia, in the forms of esophageal atresia or trachoesophageal fistula formation, can be treated with stenting. Migration, inflammation and granulation tissue and fistula formation commonly occur with long-term stenting, due mostly to the limited material types of existing stents.

Stenting has improved enormously since the 1900s when it first began. There is still much room to grow, and material science has since advanced further. From among the many advanced materials available today, type I fibrillar collagen, polycaprolactone polymer, and thermoplastic polyurethane polymer were explored for this research. The goals of this research were to demonstrate 3D-printing capability of each polymer explored, to mechanically test the resulting printed stent, and to compare these stent results to the current industry standard: silicone stents.

This research identified the potential of using FDM printing for quick, on-site manufacturing of simple stents. This indicates FDM is indeed a viable 3D printing method for polymer stent manufacturing in the future, and should be further explored. The FDM printability-analysis demonstrated medical-grade PCL can be confirmed to print under carefully maintained conditions of 120-130^{o}C, and a rate of 8mm/sec. FDM printability of TPU has been reaffirmed, and potential applications as a stent were explored mechanically. TPU results were similar to medical-grade silicone polymer.

This research contributed to furthering the advancement of stent development for tracheobronchial implantation by exploring three potential materials from which tracheal

stents can be manufactured. Stent manufacturing was undertaken using FDM printing methods. Each of the polymer materials was compared to the industry standard silicone polymer. Testing results suggest that biocompatible/bioresorbable PCL, and biocompatible/biodegradable TPU are able to handle equal or greater compressive loads than silicone before plastic deformation occurs. Collagen proto-stents that were manufactured were of 3wt% or less collagen concentration, and were not able to achieve the same load-bearing ability equal to the polymers tested.

Linear regions of stent stress-strain curves for each material were plotted and compared. Results suggest very similar behavior between TPU-based and silicone-based stents. Pure PCL showed greater elasticity than silicone, and thus was not as stiff. While the PCL compression testing was unsuccessful, the segment tested lacked equal or greater stiffness compared to silicone or TPU. Further testing, printing of a full-length PCL stent, and continuous tweaking of printing parameters for PCL may result in a PCL stent with varied elasticity, as well as a stiffer PCL stent.

This research identified the potential of using type I fibrillar collagen for stenting. Tubes were formed through injection molding 3D printing methods, yet higher collagen wt% levels and even greater levels of UV polymerized cross-linking should be explored. Analysis of collagen proto-stents demonstrated collagen tube compression loading maxima (Appendix A). Results suggest the tubes need to be made using a greater concentration of collagen to withstand the average 35kPa forces experienced by the trachea in a case of tracheomalacia. With the current collagen concentration method, it is difficult to concentrate beyond 3wt%; revisions to the protocol could be undertaken to improve this.

Overall, these results are very promising. Through this research, material printability of type I fibrillar collagen, PCL, and TPU were determined, along with tensile and compressive strengths of stents manufactured in comparison to silicone. Results suggest TPU and PCL show promise as alternatives to silicone polymer stents as an industry standard in treatment of tracheomalacia.

CHAPTER 8. FUTURE WORK

While this research presented an overview of the process of creating a stent via AM methods of FDM printing, there are still points which need addressing. First, the stents were all manufactured in the form of a simple cylindrical tube much like the Dumon stent. For our purposes this simple geometry was justified, however, more complicated stent geometries such as mesh-stents are where future research could be directed.

Continuing to adjust parameters for collagen tube stent stiffness to attempt to identify ideal material UV-polymerization levels should not be excluded from future research. As well, future studies should include additional measurements with a larger sample size of collagen tube stents over a greater range of crosslinking levels. PCL printing parameters can also, through further exploration, possibly offer stents with differing elasticity such that a slightly stiffer PCL stent, at the full of a Dumon stent, can be printed.

The present research was limited to printing of basic stent geometries and mechanically testing each stent for characterization of stent behavior, similar to tests undertaken in past research. This was done under the assumption that the materials were likely biocompatible when post-processed into stents. While justified for the scope of this research, integration of *in vitro* testing of processed materials is required to support the literature-backed assumptions upon which the findings of this research are based.

REFERENCES

[1] Ikeda, S., Hanawa, T., et al., "Diagnosis, incidence, clinicopathology and surgical treatment of acquired tracheobronchomalacia." Nihon Kyobu Shikkan Gakkai Zasshi. 1992. 30(6):1028-35

[2] Beasley SW, Qi BQ. "Understanding tracheomalacia." J Paediatr Child Health. Jun 1998. 34(3):209-10.

[3] Carden KA, Boiselle PM, Waltz DA, Ernst A. "Tracheomalacia and tracheobronchomalacia in children and adults: an in-depth review." Chest. 2005. 127(3):984-1005.

[4] Gaissert HA, Burns J. "The compromised airway: tumors, strictures, and tracheomalacia." Surg Clin North Am. Oct 2010. 90(5):1065-89.

[5] Brünings W., Albercht W., "Direkte Endoskopie der Luft- und Speisewege." Stuttgart, Enke, 1915. 134-138.

[6] Canfield N., Norton N., "Bony stenosis of the larynx." Ann Otol Rhinol Laryngol. 1949. 58:559-565.

[7] Montgomery W.W., "T-tube tracheal stent." Arch Otolaryngol. 1965. 82:320-321.

[8] Dumon J.F., "A dedicated tracheobronchial stent." Chest. 1990. 97:328-332.

[9] Freitag L., "Tracheobronchial Stents." Interventional Bronchoscopy. Prog Respir Res., Basel, Karger. 2000. 30:171-186.

[10] Chin S., Litle V., et al., "Airway Stents." Ann Thorac Surg. 2008. 85:S792-796.

[11] Dumon J.F., et al., "Seven-year experience with the Dumon prosthesis." Journal of Bronchology. 1996. 3:6-10.

[12] Bolliger C.T., et al., "Evaluation of a new self-expandable silicone stent in an experimental tracheal stenosis." Chest. 1999. 115:496-501.

[13] Häußinger K., et al., "Photodynamic therapy of inoperable patients with early stage lung cancer." Abstract World Congress for Bronchology. 1998. pp118.

[14] Monnier P., et al., "The use of covered Wallstent for the palliative treatment of inoperable tracheobronchial cancers. A prospective multicenter study." Chest. 1996. 110:1161-1168.

[15] Freitag L., et al., "Mechanical Properties of Airway Stents." Journal of Bronchology. 1995. 2:270-278.

[16] Freitag L., et al., “Theoretical and experimental basis for the development of a dynamic airway stent.” Eur Respir J.. 1994. 7:2038-2045.

[17] Sun, J., et al. “A CAD/CAM system for fabrication of facial prostheses.” Rapid Prototyping Journal. 2011. 17(4):253-261.

[18] “Additive Manufacturing: Opportunities and Constraints.” Roundtable forum, Royal Academy of Engineering. 23 May 2013.

[19] Serenó, L., et al., “New advances on tracheal stent manufacturing.” 6th IFAC Conference on Management and Control of Production and Logistics. 2013.

[20] Aktin, T., Özdemir, R.G., “An integrated approach to the one-dimensional cutting stock problem in coronary stent manufacturing.” European J of Operational Research. 2009. 196:737-743.

[21] Friel, R.J., “Power ultrasonics for additive manufacturing and consolidating of materials.” Power Ultrasonics. 2015. 13:313-335.

[22] Jerby, E., et al., “Incremental Metal-Powder Solidification by Localized Microwave-Heating and its Potenial for Additive Manufacturing.” Addit. Manuf. 2015

[23] Smith, J.A., and Seyfarth, A., “Patient-adaptable biomedical devices – Benefits and barriers for granting patients more control.” Biodevices: Proceedings of the First International Conference on Biomedical Electronics and Devices. 2008. 1:245-248.

[24] Singare S., “Individually prefabricated prosthesis for maxilla reconstruction.” Journal of Prosthodontists, 2007;17(2):135–40. [4a] Lee, M.Y., et al. “New layerbased imaging and rapid prototyping techniques for computeraided design and manufacture of custom dental restoration.” Systems, Man and Cybernetics, IEEE International Conference. 2008. 2572 - 2577.

[25] Dai, K.R, et al. “Computer-aided custom-made hemipelvic prosthesis used in extensive pelvic lesions.” Journal of Arthroplasty. 2007. 22(7): 981–6.

[26] Harrysson, O.L., et al. “Custom-designed orthopedic implants evaluated using finite element analysis of patient-specific computed tomography data: femoral-component case study.” BMC Musculoskeletal Disorders. 2007. 8(91).

[27] Wang, .Z, et al. “Fabrication of custom-made artificial semi-knee joint based on rapid prototyping technique: computer-assisted design and manufacturing.” Chinese Journal of Reparative and Reconstructive Surgery. 2004. 18(5):347–51.

[28] Vert, M., et al., “Bioresorbability and biocompatibility of aliphatic polyesters.” J Mater Sci Mater Med. 1992. 3:432–46.

[29] Woodruff, M. A., Hutmacher, D. W., “The return of a forgotten polymer—Polycaprolactone in the 21st century.” Progress in Polymer Science. 2010. 35:1217–1256.

[30] Williams, D.F., "On the mechanisms of biocompatibility". Biomaterials. 2008. 29(20): 2941–2953.

[31] Williams, D.F., "Revisiting the definition of biocompatibility". Medical Device Technology. 2003. 14(8).

[32] Zalzal GH, Grundfast KM. "Broken Aboulker stents in the tracheal lumen." Int J Pediatr Otorhinolaryngol. 1988. 16(2):125-30.

[33] Okumura, N., et al., "Experimental Study of a New Tracheal Prosthesis." Trans Am Soc Artif Intern Organs. 1991. 37:317-319.

[34] John E McClay, MD., "Laryngeal and Tracheal Stents Treatment & Management." Medscape. 2014. Associate Professor of Pediatric Otolaryngology, Department of Otolaryngology-Head and Neck Surgery, Children's Hospital of Dallas, University of Texas Southwestern Medical Center.

[35] Di Lullo, G. A.;et al., "Mapping the Ligand-binding Sites and Disease-associated Mutations on the Most Abundant Protein in the Human, Type I Collagen". J. Biol. Chem. 2002. 277(6): 4223–4231.

[36] Walters, B.D., Stegemann, J.P., "Strategies for directing the structure and function of three-dimensional collagen biomaterials across length scales." Acta Biomaterialia. 2013. 10(4): 1488-501.

[37] Ramchandran, G., Kartha G., "Structure of Collagen." Nature. 1954. 174:269-70.

[38] Ramchandran, G., "The Structure of Collagen." Nature. 1956. 177:710-1.

[39] Rich, A., Crick, F., "The Structure of Collagen." Nature. 1955. 176:915-6.

[40] Beriso, R., et al., "Crystal structure of the collagen triple helix model [(Pro-Pro-Gly)10]3." Protein Sci. 2002. 11:262-70.

[41] Forgacs, G., et al., "Assembly of collagen matrices as a phase transition revealed by structural and rheologic studies." Biophysics. 2003. 84:1272-80.

[42] Johnson, T., et al., "Tailoring material properties of a nanofibrous extracellular matrix derived hydrogel." Nanotechnology. 2011. 22:1-23.

[43] Chen, M-C., et al., "A novel drug-eluting stent spray-coated with multi-layers of collagen and sirolimus." J of Controlled Release. 2005. 108:178-189.

[44] Sekine, T., MD, et al., "Carinal Reconstruction With A Y-shaped Collagen-conjugated Prosthesis." J of Thoracic and Cardio Surg. 2000. 119(6):1162-1168.

[45] Tatekawa, Y., et al., "Tracheal defect repair using a PLGA-collagen hybrid scaffold reinforced by a copolymer stent with bFGF-impregnated gelatin hydrogel." Pediart Surg Int. 2010. 26:575-580.

[46] Hutmacher, D.W., "Scaffolds in tissue engineering bone and cartilage." Biomaterials. 2000. 21:2529–43.

[47] Wiria, F.E., et al., “Poly-e-caprolactone/ hydroxyapatite for tissue engineering scaffolds fabrication via selective laser sintering.” Acta Biomater. 2007. 3(1):1–12.

[48] Tan, K.H., et al., “Selective laser sintering of biocompatible polymers for applications in tissue engineering.” Bio-med Mater. 2005. 15(1–2):113–24.

[49] Chen, G., et al., “Silk fibroin modified porous poly-epsilon-caprolactone scaffold for human fibroblast culture in vitro.” J Mater Sci:Mater Med. 2004. 15:671–7.

[50] Oyane, A., et al., “Simple surface modification of poly(epsilon-caprolactone) to induce its apatite-forming ability.” J Biomed Mater Res A. 2005. 75A(1): 138–45.

[51] Chang, G., et al., “Physical and hydrodynmaic factors affecting erythrocyte adhesion to polymer surfaces.” J Biomed Mater Res. 1988. 22:13–29.

[52] Huang, S., “Biodegradable polymers.” Encyclopedia of polymer science and engineering. 1985. 220–43.

[53] Ginde, R., Gupta, R., “In vitro chemical degradation of poly(glycolic acid) pellets and fibers.” J Appl Polym Sci. 1987. 33:2411–29.

[54] Gopferich, A., et al., “Predicting drug-release from cylindric polyanhydride matrix discs.” Eur J Pharm Biopharm. 1995. 41:81–7.

[55] Vert, M., “Polymeric biomaterials: strategies of the past vs. strategies of the future.” Progr Polym Sci. 2007. 32:755–61.

[56] Liu, S. J, et al., “Fabrication of balloon- expandable self-lock drug-eluting polycaprolactone stents using micro- injection molding and spray coating techniques.” Ann Biomed Eng. 2010. 38: 3185-94.

[57] Liu, Kuo-Sheng, M.D., et al., “Experimental absorbable stent permits airway remodeling.” J of Thoracic and Cardiovascular Surgery. 2010. 141-2:463-468.

[58] Chen, J., et al., “Carbon nanotube network structure induced strain sensitivity and shape memory behavior changes of TPU.” Materials & Design. 2015. 69:105-113.

[59] Kim, B.K., et al., “Polyurethanes having shape memory effects.” Polymer. 1996. 37:5781-5793.

[60] Huang, W.M., et al., “Thermo-moisture responsive polyurethane shape-memory polymer and composites: a review.” J Mater Chem. 2010. 20:3367-3381.

[61] Bartolomé, L., “The Influences of deformation state and experimental conditions on inelastic behavior of an extruded thermoplastic polyurethane elastomer.” Materials & Design. 2013, 49:974-980.

[62] Varela, J., et al., “Mechanical properties of a new thermoplastic polymer for orthodontic archwire.” 2014.

[63] Fernández, J., et al., “Effects of chain microstructures on mechanical behavior and aging of PLCL biomedical thermoplastic elastomer.” J of the Mechanical Behavior of Biomed Mat. 2012. 12:29-38.

[64] “Moisture Absorption: Thermoplastic Composites.” Fiberforge. 2008.

[65] Van de Velde, et al., “Thermoplastic polymers: overview of several properties and their consequences in flax fibre reinforced composites.” Polymer Testing. 2001. 20:885-893.

[66] Theron, J.P., et al., “Modification, crosslinking and reactive electrospinning of thermoplastic-medical-polyurethane for vascular graft applications.” Acta Biomaterialia. 2010. 6:2434-2447.

[67] Hernandez-Ortiz, J.P., Osswald, T.A., “Modeling processing of silicone rubber: liquid versus hard silicone rubbers.” J. Appl. Polym. Sci. 2010. 119:1864-1871.

[68] Rey, T., et al., “Influence of the temperature on the mechanical behaviour of filled and unfilled silicone rubbers.” Polym. Test. 2013. 32:492-501.

[69] Freitas, M.S., et al., “Thermal model for curing implantable silicone in the moulding process applied to tracheal stents.” Applied Thermal Engineering. 2015. 75:1001-1010.

[70] Meredith I.T., et al., “Primary Endpoint Results of the EVOLVE Trial: A Randomized Evaluation of a Novel Bioabsorbable Polymer-Coated, Everolimus-Eluting Coronary Stent.” J Am College of Cardiology. 2012. 59, 15:1362-1370.

[71] Bracci, R., M.D., “Bioresorbable Airway Splint Created with a Three-Dimensional Printer.” N Engl J of Med. 2013. 368:21.

[72] “Select Updates for Non-Clinical Engineering Tests and Recommended Labeling for Intravascular Stents and Associated Delivery Systems.” U.S. Department of Health and Human Services, Food and Drug Administration, Center for Devices and Radiological Health. 2010. <http://www.fda.gov/medicaldevices/deviceregulationandguidance/guidancedocuments/ucm071863.htm>

[73] Bartolo, P.J., Gaspar, J., “Metal filled resin for stereolithography metal part.” CIRP Annals – Manufacturing Technology. 2008. 57:235-238.

[74] Yeong, W-Y, et al., “Rapid prototyping in tissue engineering: challenges and potential.” Trends in Biotechnology. 2004. 22(12):643-652.

[75] Freitag, L., et al., “Theoretical and experimental basis for the development of a dynamic airway stent.” European Respiratory Journal. 1994. 7(11): 2038-2045.

[76] Freitag, L., et al., “Mechanical properties of airway stents.” Journal of Bronchology & Interventional Pulmonology. 1995. 2(4): 270-278.

[77] Vearick, S. B., et al., “Development and in vivo testing of a Nitinol tracheal stent.” Journal of Biomedical Materials Research Part B: Applied Biomaterials. 2007. 83(1): 216-221.

[78] Instamorph Polycaprolactone (hobbyist grade); <https://www.instamorph.com/about>.

[79] Sigma-Aldrich Polycaprolactone;
<http://www.sigmaaldrich.com/catalog/product/aldrich/181609?lang=en&region=US&gclid=CNLnjcCnocUCFRc8gQodh50Aqw>.

[80] Ninjaflex Thermoplastic Polyurethane –colorless, or "water";
<http://www.fennerdrives.com/ninjaflex3dprinting/_/3d///>.

[81] Saito (MD) et al., "New tubular bioabsorbable knitted airway stent- biocompatibility and mechanical strength." J of Thor & Cardio Surg-General Thoracic Surgery. 2002. 123(1): 161-167.

[82] Wang, J. et al., "Fully Biodegradable Airway Stents Using Amino Alcohol-Based Poly(ester amide) Elastomers." Adv Healthc Mater. 2014. 2(10): 1329-1336.

[83] Bhat, S. V. "Synthetic Polymers." Biomaterials. 1st ed. Springer Verlag, 2014. 69. Print.

[84] Eshraghi S., and Das, S., "Mechanical and Microstructural Properties of Polycaprolactone Scaffolds with 1-D, 2-D, and 3-D Orthogonally Oriented Porous Architectures Produced by Selective Laser Sintering." Acta Biomater. 2010. 6(7): 2467-2476.

[85] Thermoplastic Polyurethane Elastomers (Elastollan – Material Properties), PU Solutions Elastogran. Technical Information. BASF (The Chemical Company), 2011. 07. Print.

[86] ASM Materials for Medical Devises Database Committee, "Materials and Coatings for Medical Devices: Cardiovascular." ASM International. 2009. 297-303. Print.

[87] Melgoza, E. L., et al., "An integrated parameterized tool for designing a customized tracheal stent." Computer-Aided Design. 2012. 44: 1173-1181.

[88] Neppalli, R., et al., "Improvement of tensile properties and tuning of the biodegradation behavior of polycaprolactone by addition of electrospun fibers." Polymer. 2011. 52: 4054–4060.

[89] Huo, J., et al, "Parametric elastic analysis of coupled helical coils for tubular implant applications: Experimental characterization and numerical analysis." J of Mech Behav of Biomed Mater. 2014. 29: 462-469.

APPENDIX A. COLLAGEN TUBE DATA

Collagen Tube Data in collaboration with Senior Design Group "A'ris Bioinnovations": George Plasko, Olivia Tran, Ryan Dingman, and Heidi Martin)

Figure A.1. 0.5 wt% collagen

Figure A.2. 0.83 wt% collagen

Figure A.3. (a and b) 0.77 wt% collagen

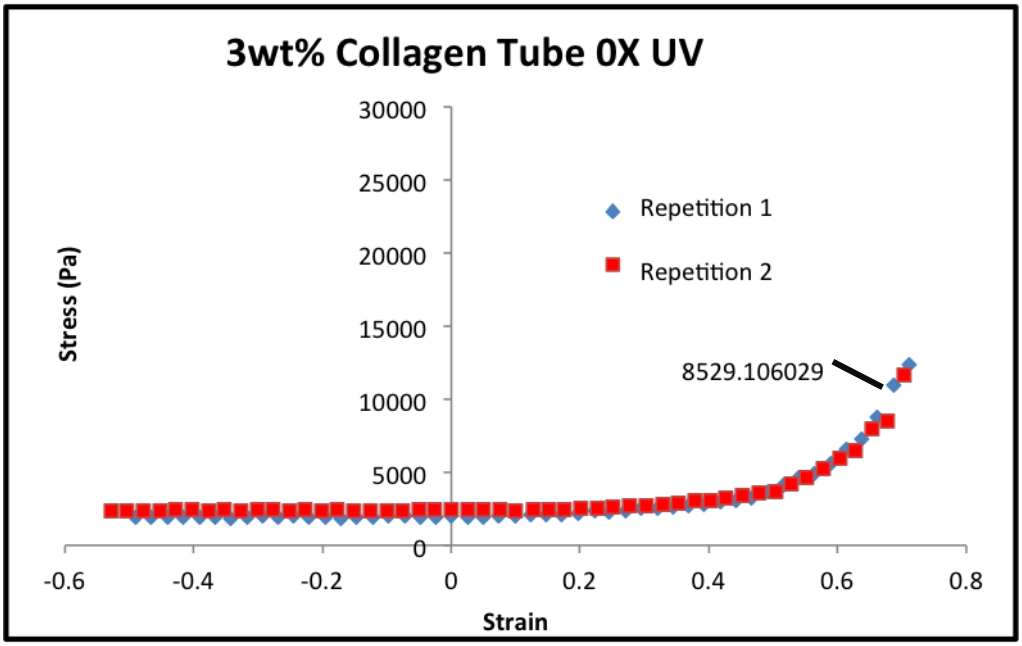

Figure A.4. Rheometer results for un-UV-cross-linked collagen. Two samples were used, entered irreversible deformation around strain levels of 0.678, and a stress of approximately 8,529Pa. A tracheomalacial patient's trachea experiences approximately 35kPa of stress on average.

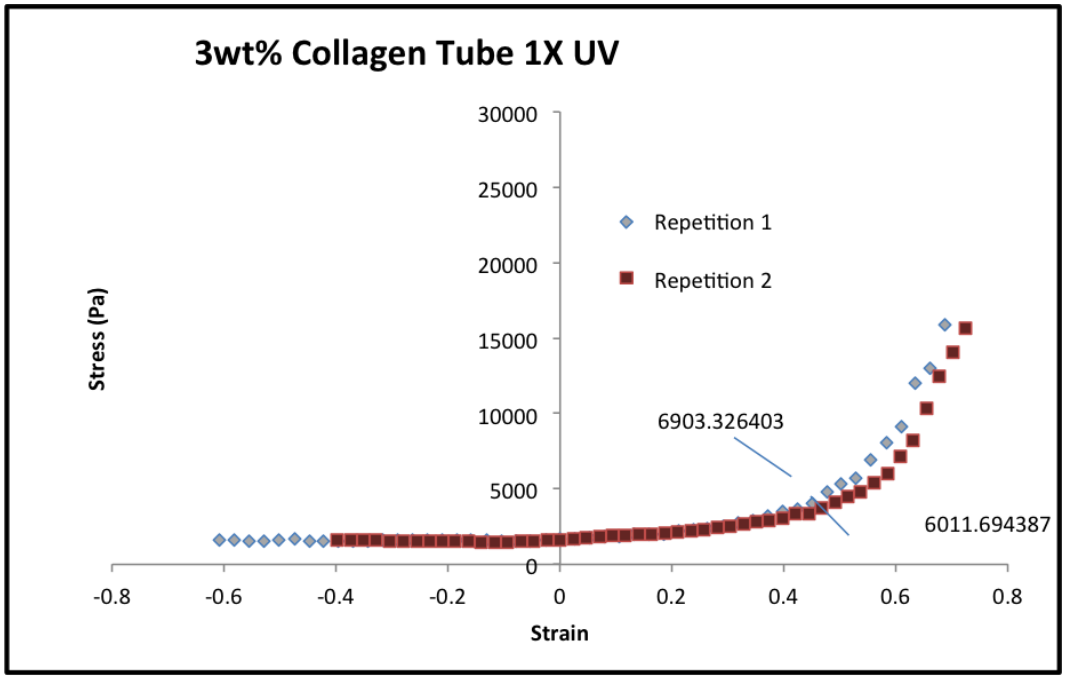

Figure A.5. Rheometer results for collagen UV cross-linked for 1 burst of 750J, i.e. "weakly cross-linked". Plastic deformation occurred after stresses of 6903Pa and strain levels reached 0.556 for the first repetition, and after stresses of 6011Pa with strain levels of 0.585 for the second repetition. Being closer to the 35kPa the trachea exerts, the material may not fail if stresses experienced by the proto-stent are adequately distributed.

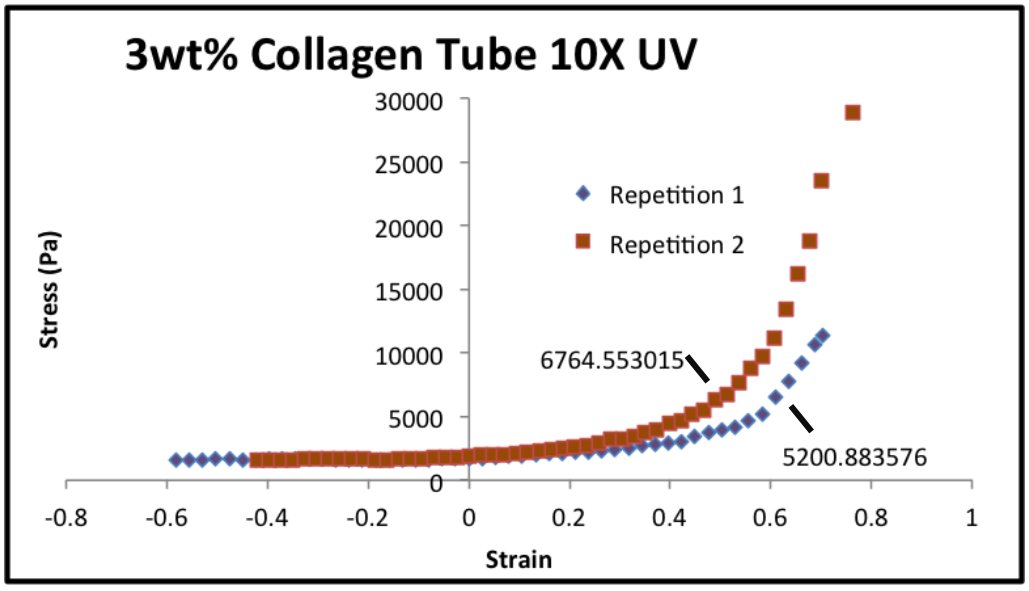

Figure A.6. Rheometer results for collagen UV-cross-linked for 10 bursts @ 750J each, or "slightly more cross-linked"/"moderately cross-linked". Both samples underwent plastic deformation close to 0.5 strain levels. The collagen disc for repetition 1 withstood approximately 5201kPa of compressive force, while the disc for repetition 2 withstood about 6765kPa of force. Again, pressures exerted by the trachea must be dispersed across the stent, as localized force would likely result in collapse of the collagen proto-stent.

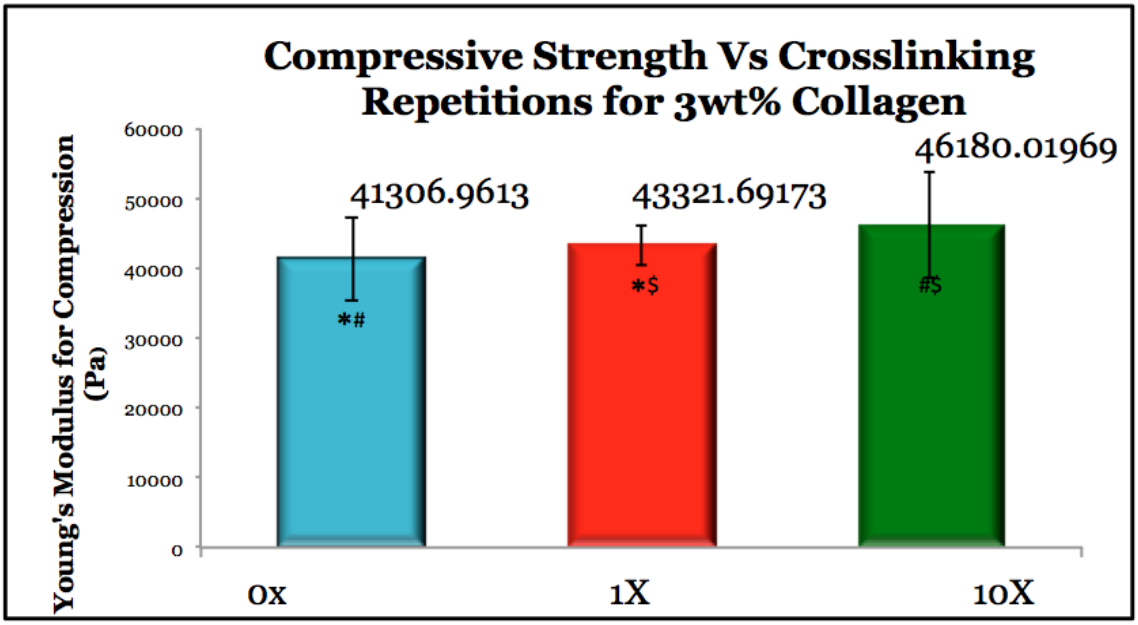

Figure A.7. Compressive modulus testing comparing all collagen stents at 3 wt% concentration. Where *=(-39089.20, 43118.66), #=(-38405.64, 28659.52), $=(-40625.24, 34908.59). No significant difference is displayed between the varying lower levels of UV cross-linking.

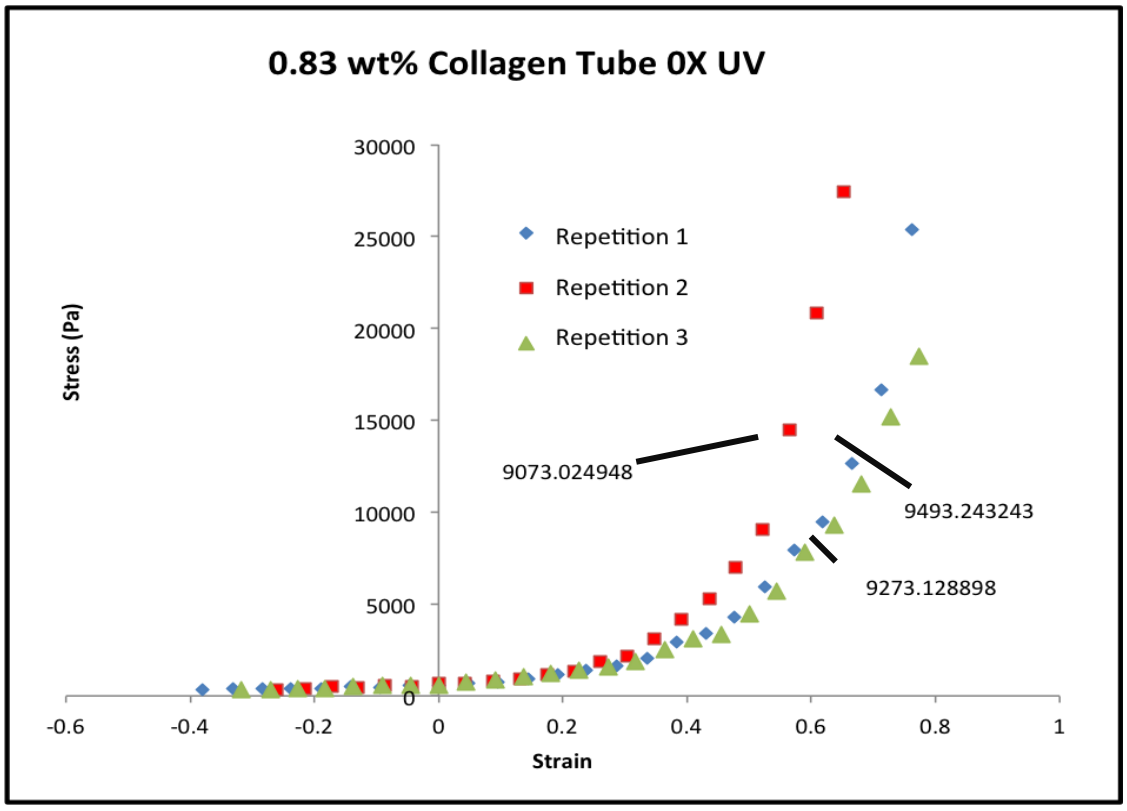

Figure A.8. Results of compression repetition on collagen that has not been UV-cross-linked. Despite greater collagen concentration percentage, lack of UV polymerization leaves maximal compressive forces of 9,073Pa for the first repetition, 9,493Pa for repetition 2, and 9,273Pa for repetition 3. These proto-stents would not withstand average tracheal forces experienced by a tracheomalacial patient.

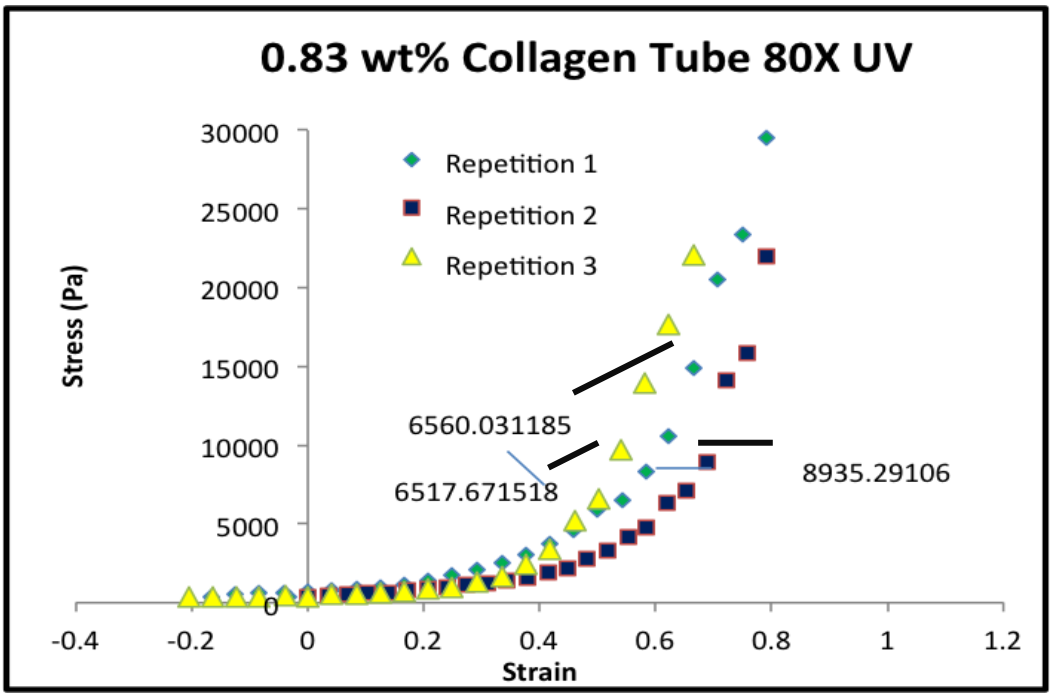

Figure A.9. Results of compression repetition on collagen tube discs after 80 bursts of UV cross-linking. Despite higher UV polymerization and more concentrated collagen wt%, the maximal stress values for each repetition are less than 35kPa, possibly resulting in cyclic failure if stresses experienced are not evenly distributed throughout the stents.

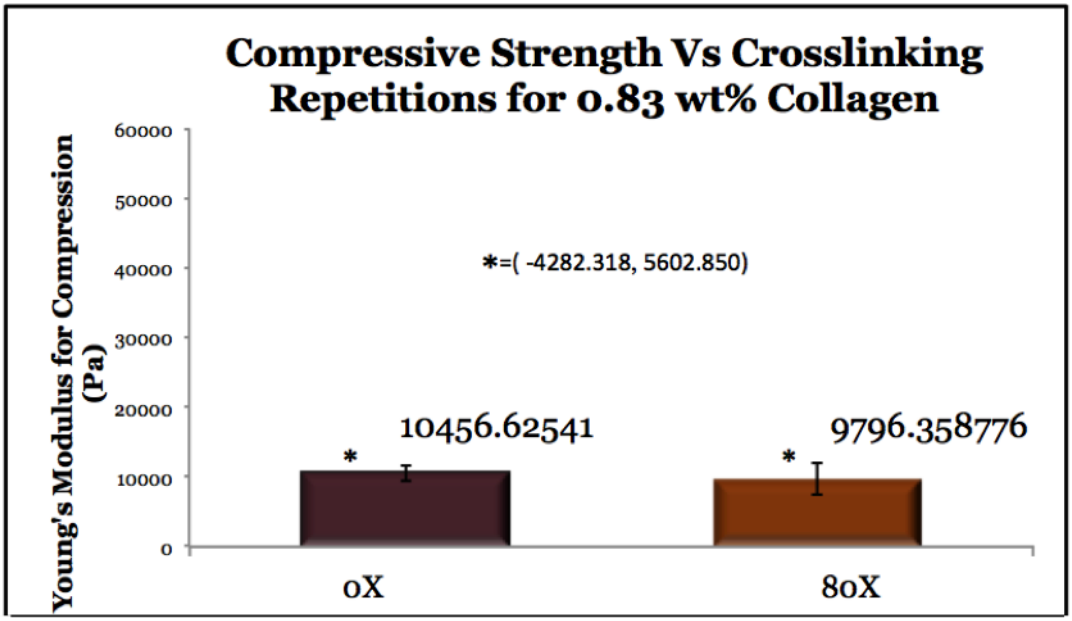

Figure A.10. Amount of cross-linking vs. compressive strength of the 0.83 wt% stent. Higher cross-linking of a more concentrated collagen percentage, compared to an uncross-linked stent of that same concentration, surprisingly resulted in little difference of compressive strength.

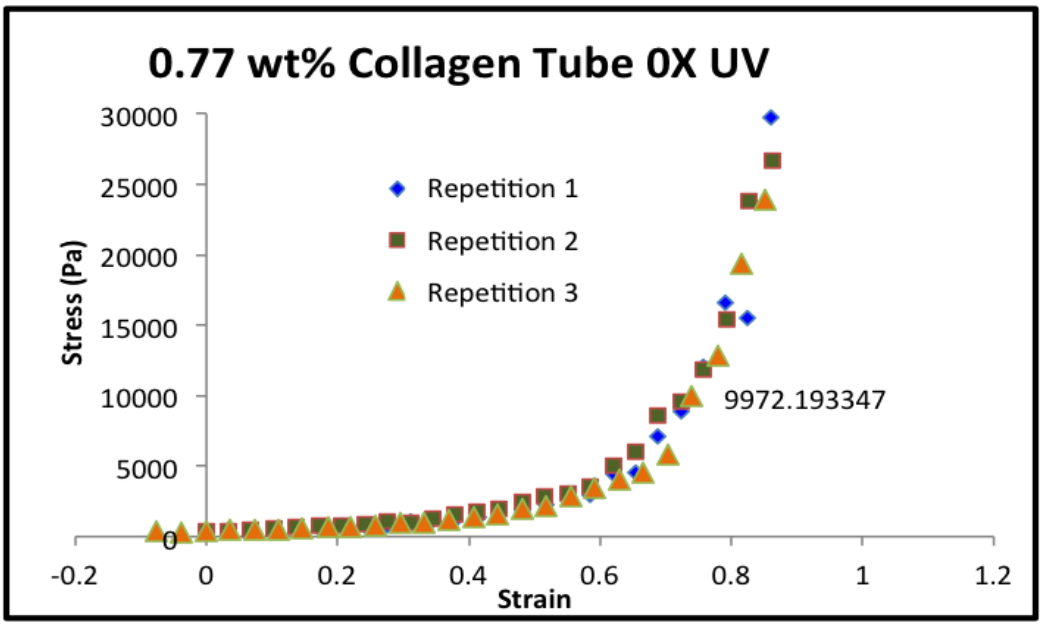

Figure A.11. Results of compression on mid-to-high collagen concentration that is not UV cross-linked. Plastic deformation occurs at a strain level of 0.73, with stress values at about 9,972Pa. Again, compared to the average 35kPa stress exhibited on a tracheomalacial patient's airways, 27% of this level of pressure applied locally would likely cause this collagen proto-stent to collapse.

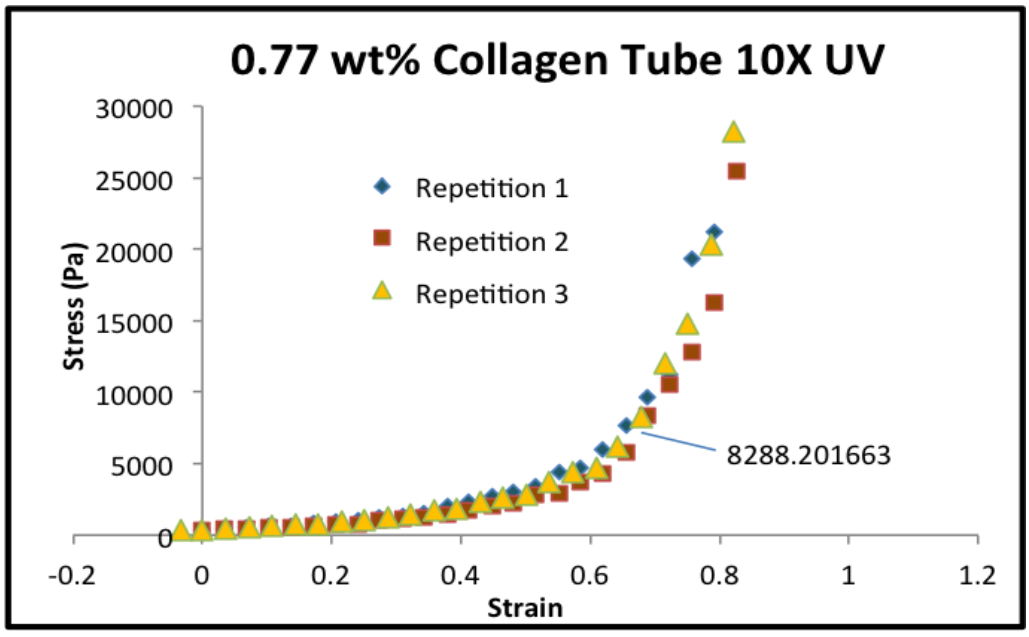

Figure A.12. Results of compression testing for a mid-to-high collagen concentration wt% stent that underwent 10 bursts of UV cross-linking. As the stents begin to deform after 8,288Pa of stress, at approximately 23.68% of the total radial pressure a tracheomalacial patent's tracheal wall would exert during exhalation (35kPa) this stent with low-level UV polymerization could collapse.

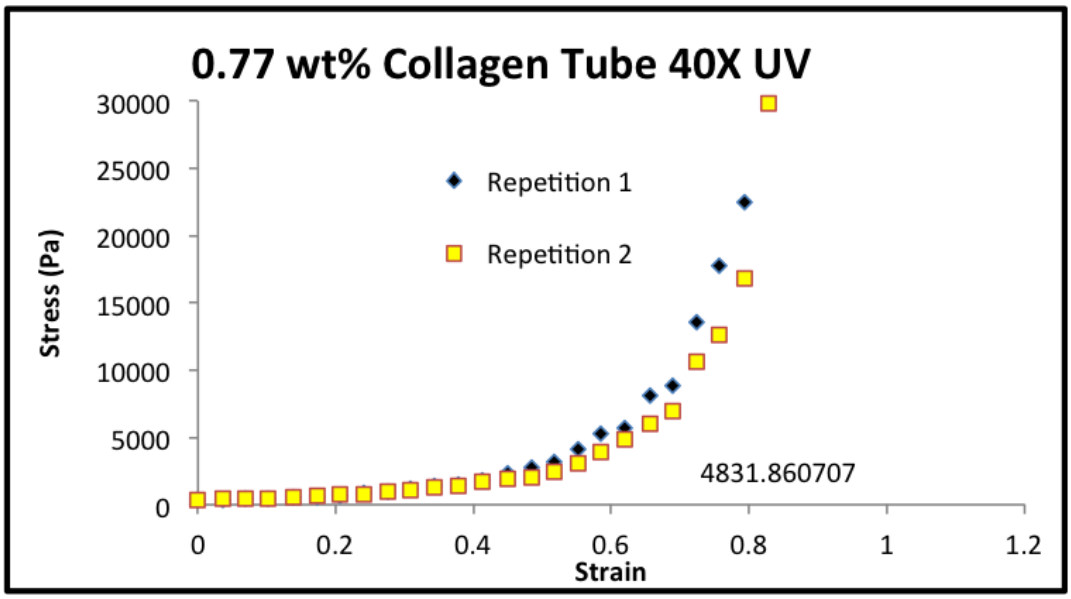

Figure A.13. Results of compression repetition for a mid-to-high collagen concentration stent that underwent 40 bursts of UV cross-linking. Surprisingly, compression testing revealed that these collagen discs were weaker than those that were UV polymerized at only 10 bursts. This could, however, be due to slight damage to the collagen discs prior to testing.

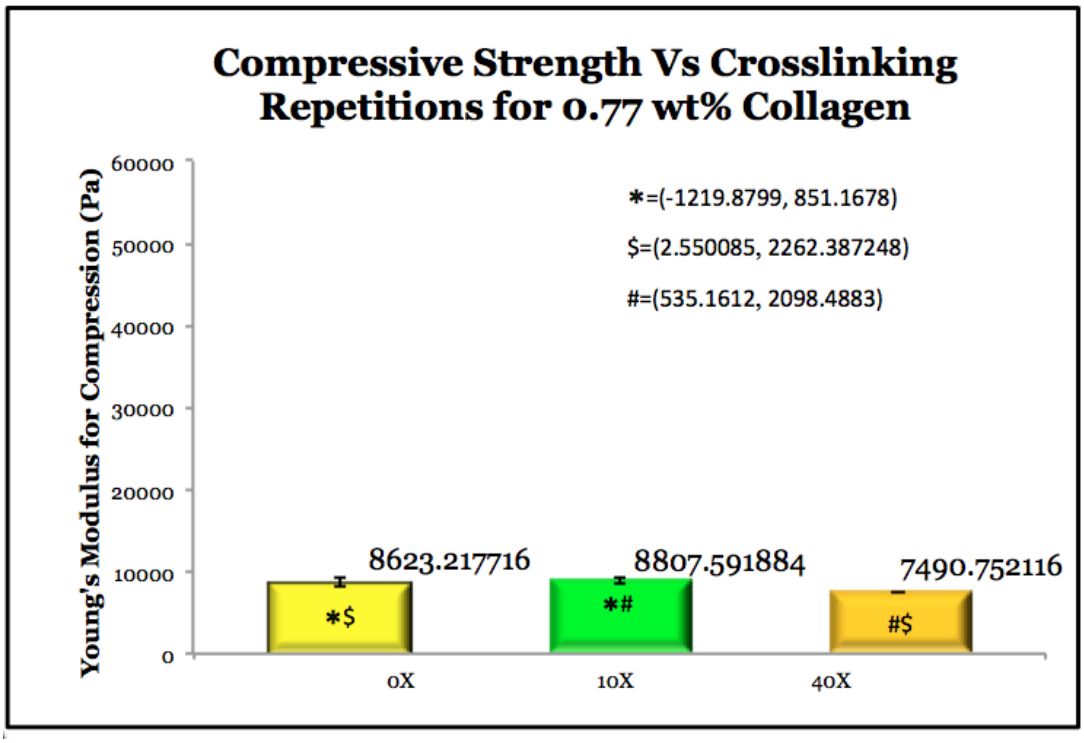

Figure A.14. Comparing all the results for 0.77 wt% collagen discs. It is likely that slight damage to the 40X collagen discs prior to testing resulted in weaker stress-strain values than the 10X collagen discs. Again, there was no significant variation between strengths at this collagen concentration.

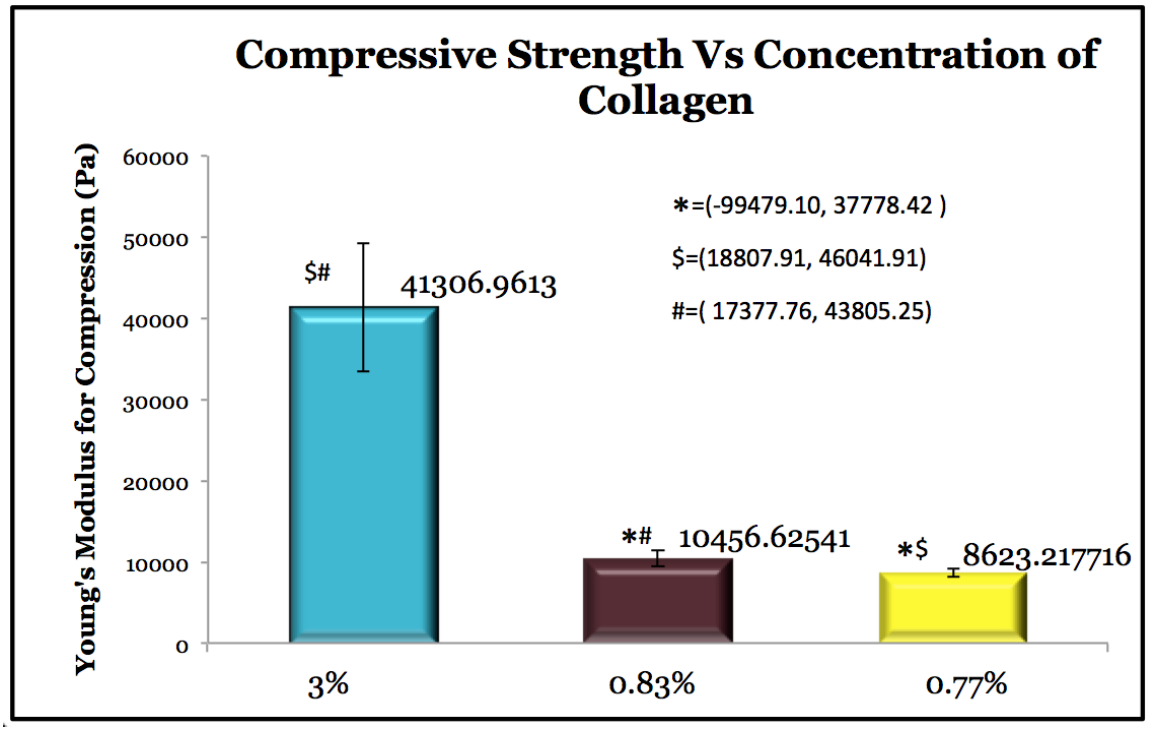

Figure A.15. Comparing all collagen concentration percentage results. Expectedly, the highest collagen concentration had the greatest compressive strength. There was little difference between collagen concentrations <1% wt.

Collagen Preparation Procedure
(Provided by Dr. Mike Yost's Lab)

Collagen is prepared from hide of an 18-month-old bovine steer (Caughman's in Lexington, SC)

1. Cut hide into 4x6 cm strips and freeze prior to processing.

2. Remove all superficial epidermis including the hair and follicle pits. Depending on the hide, hair clippers may be needed to cut hair off first.

3. Wash collagen with running tap water to remove all hair.

4. Incubate collagen overnight at 4^{o}C in the fridge, in 2% $Ca(OH)_2$ solution per hide weight (lime water). Mix well and place in tumbler. Incubate at 4^{o}C in the fridge.

5. Wash the collagen under running water. The collagen is placed in 1M NaCl solution and left at 4^{o}C in the fridge. The solution pH should be brought to 5 with 1M HCl solution.

6. After the pH remains stable at 5, wash the collagen in DI water until water is clear and the conductivity is at 100μS/cm to make sure all the salt is washed out. If not going to process right away, freeze it.

7. Thaw out the de-limed collagen, or continue processing. Cut the hides into 1 inch square pieces.

8. Put the collagen in cold 0.5M CH_3COOH (acetic acid) solution. Then add pepsin (50:1 hide weight to pepsin ratio). Incubate overnight at 4^oC in the fridge.

9. Clean the meat grinder well to remove any rust. Place lard to lubricate. Run ice through the grinder until it comes out clean. Add 2 pieces of hide, followed by a half handful of ice. Wait until it comes out. Repeat it until all the collagen is grinded. Collect the collagen in a stainless steel bowl.

10. After the collagen has been ground, add cold 0.5M CH_3COOH (acetic acid) solution. Mix in the kitchen aid mixer until you reach a soupy consistency. Gradually add acetic acid while mixing until you get the right consistency. Use 1M HCl to bring the pH down to 3-4.5, or a lower pH if necessary. Incubate overnight at 4^oC in the fridge.

11. The next day, check the pH and adjust to a pH 3 as needed.

12. Clean the press. Put the collagen pieces through the press. The mesh filter must be cleaned with hot water frequently to avoid clogging.

13. Add cold 0.5M CH_3COOH (acetic acid) to the pressed collagen and mix well until liquid. Measure how much acid is added to the collagen.

14. Add 1M NaCl (taking into account the amount of acetic acid that was added in step 13) until the collagen comes out of solution. Up to 2M NaCl can be added. Incubate overnight at 4^oC in the fridge.

15. The next day, spin down the collagen to get rid of the water at 5000-7000 rpm for 30 minutes at 4^oC. It will take several spins to collect all of the collagen. Make sure the collagen is kept cold at all times. ******When all sides of centrifuge are weighted, collagen collection works best.

16. After collecting the collagen, add ice water and adjust the pH to 5.5 with 1M NaOH. A large amount will have to be used to bring the pH up.

17. Once the pH is around 4, incubate overnight at 4^oC in the fridge.

18. The next day, adjust the pH to 5.5. The solution must have enough volume to put into dialysis tubing. Place the dialysis tubes containing the collagen into beakers of cold water and store at 4^{o}C in the fridge.

19. Keep changing the water at least twice a day for several days until the conductivity reads 50μS/cm.

20. Once the conductivity has reached the desired value, remove the collagen from the dialysis bags and transfer it to 50 mL conical tubes to freeze at -20^{o}C.

Collagen Concentrating Procedure

1. Determination of collagen concentration as:

(Dry collagen /wet collagen) x 100

2. Raw collagen was placed in a conical centrifuge tube to be spun down at 4000 rpm for 30 minutes until all collagen is collected at the bottom of the tube.

3. Excess water was removed in addition to any diluted collagen floating on the top. Concentrated collagen was stored overnight at 4^{o}C in the fridge.

a